

CHAPTER 1

INTRODUCTION

1.0 INTRODUCTION

In the agrochemical industry, fertilizers are one of the most important products. This is due to the fact that they are added to soil to release nutrients necessary for plant growth (Akelah, 1996). About half of the applied fertilizers, depending on the method of application and soil condition is lost to the environment, which results in the contamination of water (Omar, 1989). According to Malhi et al (2001), nitrogen in soil is subjected to volatilization losses which increase with factors such as high air and soil temperatures and wind speed.

One method to effectively reduce losses of nutrient components is the use of slow-release fertilizers. These fertilizers may be produced as chemically or physically prepared slow-release fertilizers (Pipko, 1988). Sulfur-coated urea (SCU) technology was developed in the 1960s and 1970s by the National Fertilizer Development Center. Sulfur was chosen as the principle coating material because of its low cost and its value as a secondary nutrient (Sartain, 2010). Sulfur is an interesting coating material as it is water impervious, can be used as a micronutrient with an important role in the development of many plants, economical and abundant industrial residue (Ayub et al, 2000).

Controlled-release fertilizers demonstrate many advantages over the conventional type, such as decreased rate of removal of the fertilizer from the soil by rain or irrigation water, sustained supply of minerals for a prolonged time, increased efficiency of the fertilizer, lower frequency of application in accordance with normal crop requirement, minimized potential negative effects associated with over dosage, and reduced toxicity (Tomaszewska and Jarosiewicz, 2002). The method of production of physically prepared slow-release fertilizers has been described in many papers. A general idea is to provide granules of water-soluble fertilizers with an insoluble coating (Pipko, 1988).

Meisen and Marthur (1978) verified the possibility of using the spouted bed for coating urea with sulfur and concluded that the product quality is a function of air temperature. Spouted beds have been developed into an effective alternative to fluidized beds for handling coarse particles, particles which exceed about 1 mm in diameter (Epstein and Grace, 1984). Applications include drying, coating, granulation, solidification and chemical reaction. Although fluidized bed spray granulation has been known and used in the industry for several years, and a number of investigations have been focused on the identification of the factors affecting the granulation process, there have been no studies conducted particularly on the relationship between these factors and the product properties (Link and Schlünder, 1997).

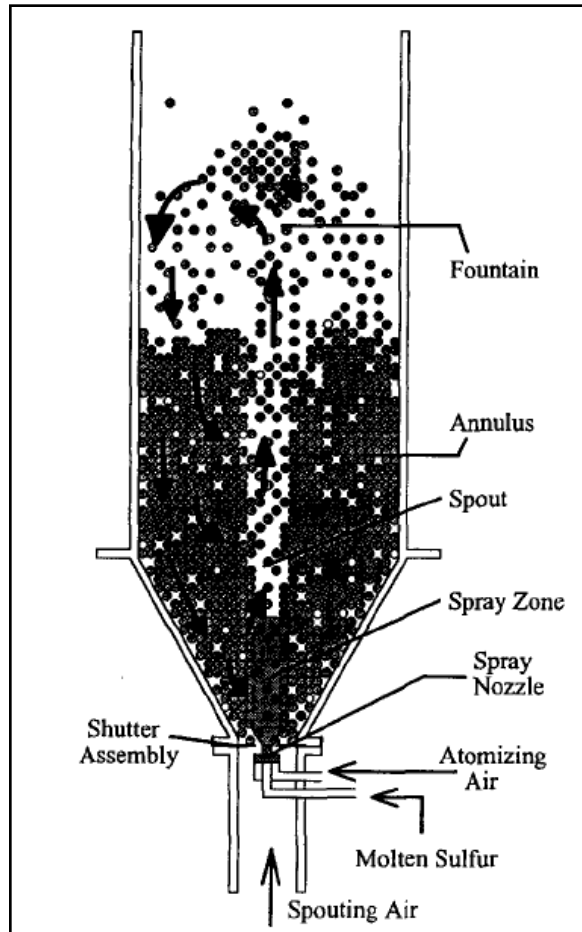


Figure 1.1: Schematic diagram of spouted bed coating unit for producing sulfur coated urea by Choi and Meisen (1996)

According to Turton (2008), the most important parameter associated with coating operations is the uniformity of the applied coating. There are two types of coating, namely, mass coating uniformity and uniformity associated with coating morphology. Situations arise in which the morphology of the coat plays a very important role in the quality control of coated products. Two coated particles might have identical amounts of coating on them but if for some reason the coating on one particle is not conformal or does not provide complete coverage, then enteric protection would not be afforded.

Imperfections in the coating film can create significant variability in the desired performance of a coat but may not be related to mass coating variability.

There are several modeling techniques that can quantify important processing variables and are applicable to all coating processes; one of them is computational fluid dynamics (CFD). In order to predict the droplet spreading behavior on the surface of urea particle, CFD will be used to simulate this phenomenon.

1.1 Objectives and Scope of Study

1. To simulate the spreading behaviour of sulfur droplet on different surface roughness with no penetration.
2. To study the effect of different surface roughness on the spreading behaviour of sulfur droplet.
3. To study the effect of contact angle and impact velocity on the spreading behaviour of sulfur droplet.

CHAPTER 2

LITERATURE REVIEW

2.0 LITERATURE SURVEY

The basic concept of controlled-release or slow-release fertilizers is that they release their nutrient contents at more gradual rates that permit maximum uptake and utilization of the nutrient while minimizing losses due to leaching, volatilization or excessive turf growth (Sartain, 2010). Generally, particles of urea were coated in two-dimensional spouted bed. The experiments were planned with the objective of verifying the influences of flow rates of sulfur and atomized air and the temperature of the air used in the spouted bed on the quality of the coated particle surface (Ayub et al, 2000). However, it is important to know that the surfaces of urea particles are rough and uneven. This becomes a major challenge to investigate the droplet spreading behavior of sulfur on the surface of urea.

2.1 History of Sulfur Coated Urea

Initial work on sulfur coating of urea was performed by Rindt et al (1968), who developed a batch-wise process in which the urea was placed in a rotary pan and sprayed with molten sulfur. The product quality was tested by determining the dissolution of 2g of sample in 10ml of water at 37.8°C after one and five days. They found that the product quality was strongly influenced by the temperatures of molten sulfur, atomizing air, and substrate of coating operation. At lower temperature, the coating was rough and difficult to seal because of premature freezing of sulfur droplets. However, at higher temperatures, the sulfur did not solidify rapidly enough and ran off the substrate.

In 1975, Marthur and Meisen designed and operated spouted bed coating process. A bed of urea was spouted with warm air while sulfur is melted in a heated vessel and forced by compressed nitrogen to an air atomized nozzle. The influences of the following variables on product quality was studied; size of urea granules, coating time, cooling time and type of cooling.

Redesigning the spouted bed coating facility overcame the major difficulties (Weiss, 1981). Blockages in the sulfur lines due to impurities or uneven heating were eliminated by filtration and temperature controls for the atomizing air and spouted bed were also operated satisfactorily. He had also studied the spreading of sulfur droplets on the urea surface which depended on the bed temperatures.

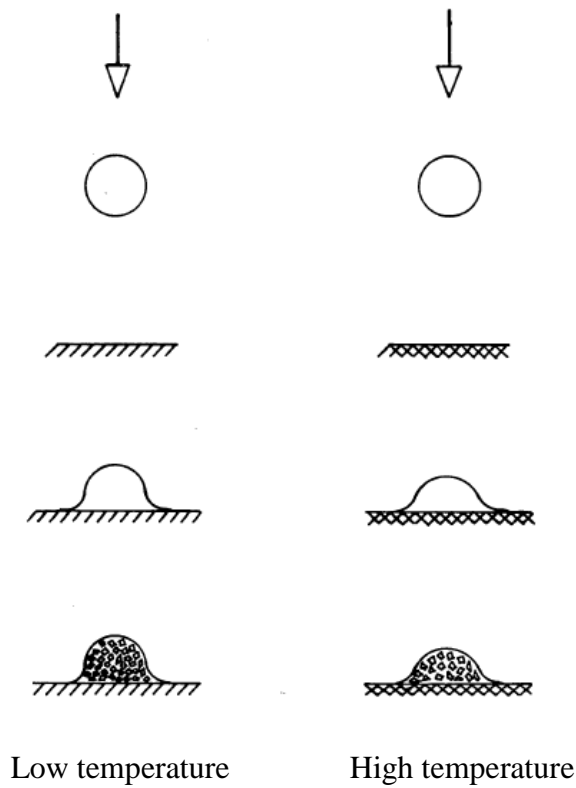


Figure 2.1: Deposition of sulfur onto urea surface at low temperature and high temperature (Weiss, 1981)

Weiss (1981) observed that when a second layer is formed by sulfur droplets impinging on the previous layer, high temperature assist the sulfur to flow into the cracks between the sulfur crystals. He concluded that elevated temperatures should improve the product quality. However, there is still lack of understanding on the spreading behavior of liquid droplet on the surface of urea particles. It should be noted that pores in the urea granules are difficult to seal due to the fact that the droplets are not able to penetrate deeply.

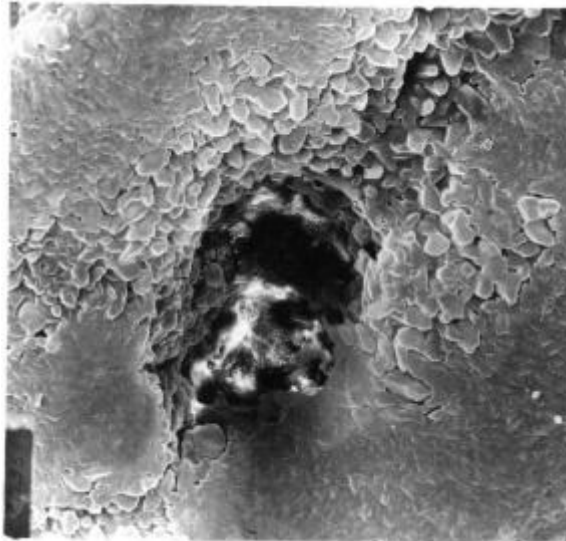


Figure 2.2: Pore in sulfur coating, 400x (Weiss, 1981)

2.2 Droplet Spreading Behavior: Experimental Approach

One of the most important parameters for sulfur to uniformly spread on the surface of the urea is the temperature. According to Choi and Meisen (1996), before sulfur is introduced into the fluidized bed, it is heated to approximately to 150°C in its tank by increasing the nitrogen pressure. This is also agreed upon by Gullett et. al (1987) in their invention of sulfur-coated urea by reducing the amount of sulfur used to coat the urea as well as by Goertz et. al (1993) in their invention of preparation of sulfur coated fertilizers process. One of their process variables is the temperature of sulfur which ranges from a limit of 290-310°F and their most preferred limit is 300°F (148.89°C) which would produce a sulfur coating of 15 to 16 weight percent. However, in a report on freeze coating process for producing sulfur-coated urea by Lee and Meisen (1983), they concluded that a lower sulfur temperature of 130-144°C will give higher weight percent coating of sulfur on the urea as can be seen in Table 2.1 and is graphically shown in Figure 2.3.

T _{sulfur} (°C)	Sulfur coating (wt%)
132	36.0
134	36.0
136	34.5
138	32.6
140	30.6
142	28.6

Table 2.1: Coating weight of molten sulfur as a function of sulfur temperature
(Lee and Meisen, 1983)

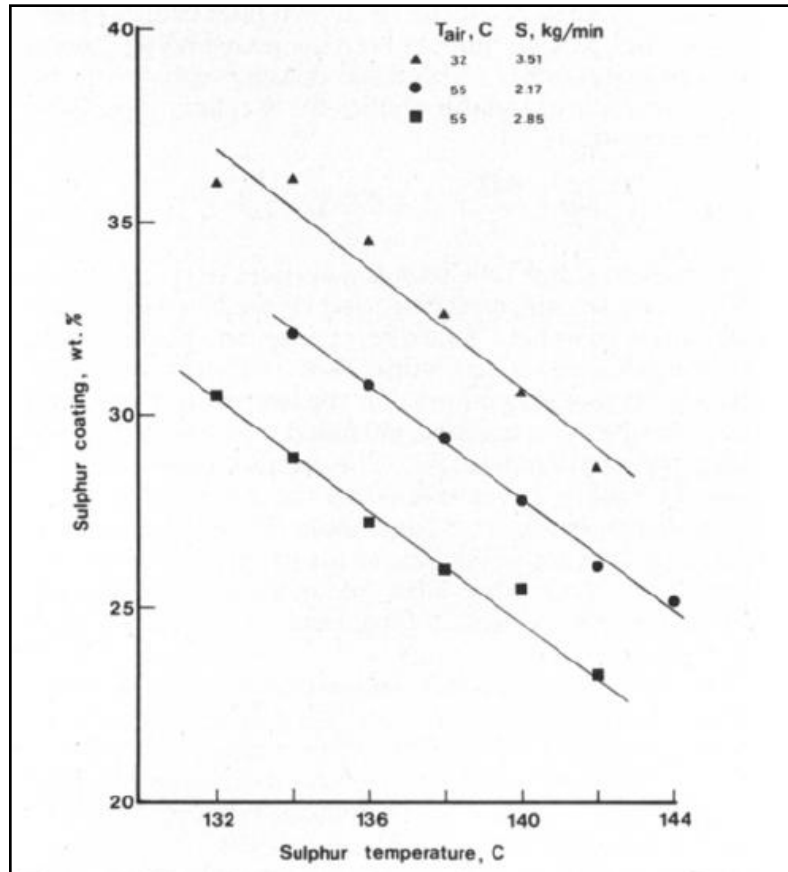


Figure 2.3: Effect of air temperature and sulfur flow rate on sulfur coating weight at different sulfur temperatures (Lee and Meisen, 1983)

In another report by Shirley and Meline (1975) for sulfur-coated urea in a 1-ton-per-hour pilot plant, they mentioned that the best temperature for sulfur spraying is approximately 310°F (154.44°C) as test have shown that the effectiveness of coating reduces as temperature decrease. However, at a temperature above 318°F, the viscosity of sulfur is so great that fine sulfur atomization is impossible to achieve. An additional important parameter to consider is the temperature of urea which needs to be preheated to a temperature of 145-150°F as insufficient pre-heated urea would result in crusty appearance and high dissolution rate of urea.

Drop impact is of interest in agriculture and scattering of pesticides is the first example. Splashed pesticides droplet can be blown away and creates pollution in nearby places. If the spreading and splashing behavior of pesticides is known, the quantity use can be reduced and pollution can be prevented (Range and Feuillebois, 1998). This same droplet spreading behavior is also seen in the coating process of urea particles to produce controlled-release urea and the impact of it to the environment as well as the quantity used.

In 1996, Range and Feuillebois studied the influence of surface roughness on liquid drop impact. They used different types of rough plates; plates with random profile of roughness, plates with regular grooves and plates with equal cavities. They observed that the splashing behavior is more dramatic on the plates with regular grooves. Results of their experiment are shown in Figure 2.4.

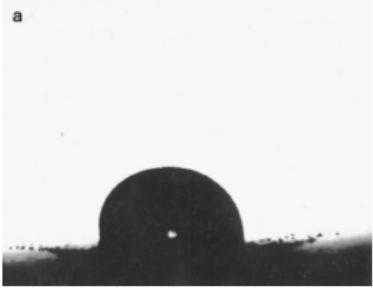

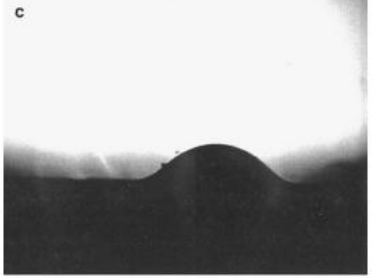

Experiment results	Description
 <p>A black and white photograph showing a water droplet impact on a smooth surface. The droplet has spread into a flat, circular shape with a very thin, uniform layer. The label 'a' is in the top left corner.</p>	<p>Water drop impact on commercial aluminum plate. Roughness, $R_a = 0.4365 \mu\text{m}$; Impact velocity = 3.54 m/s</p>
 <p>A black and white photograph showing a water droplet impact on a surface with small, uniform cavities. The droplet has spread, but there is a noticeable splash and some liquid is being ejected from the edges. The label 'b' is in the top left corner.</p>	<p>Water drop impact on Plexiglass with equal cavities. Roughness, $R_a = 12.5585 \mu\text{m}$; Impact velocity = 2.16 m/s</p>
 <p>A black and white photograph showing a water droplet impact on a surface with rectangular grooves. The droplet has spread, but there is a noticeable splash and some liquid is being ejected from the edges. The label 'c' is in the top left corner.</p>	<p>Water drop impact on Plexiglass with rectangular grooves. Roughness, $R_a = 20.170 \mu\text{m}$; Impact velocity = 2.16 m/s</p>
 <p>A black and white photograph showing a water droplet impact on a surface with triangular grooves. The droplet has spread, but there is a noticeable splash and some liquid is being ejected from the edges. The label 'e' is in the top left corner.</p>	<p>Water drop impact on Plexiglass with triangular grooves. Roughness, $R_a = 23.053 \mu\text{m}$; Impact velocity = 2.16 m/s</p>

Figure 2.4: Experimental results of different surface roughness on liquid droplet impact (Range and Feuillebois, 1998)

Katagiri et al (2005) studied the spreading behavior of an impacting drop on a structured rough surface. The rough surfaces are specially prepared with a regular pattern of surface asperities. The major physical parameters that influence the drop impact process are the size and velocity of the drop prior to the impact, the liquid properties of the drop, and the surface characteristics of the solid surface. The drop parameters are grouped in terms of non-dimensional numbers such as the Weber number, We ; the ratio of inertial to surface tension forces, and the Ohnesorge number, Oh ; the ratio of viscous to surface tension forces.

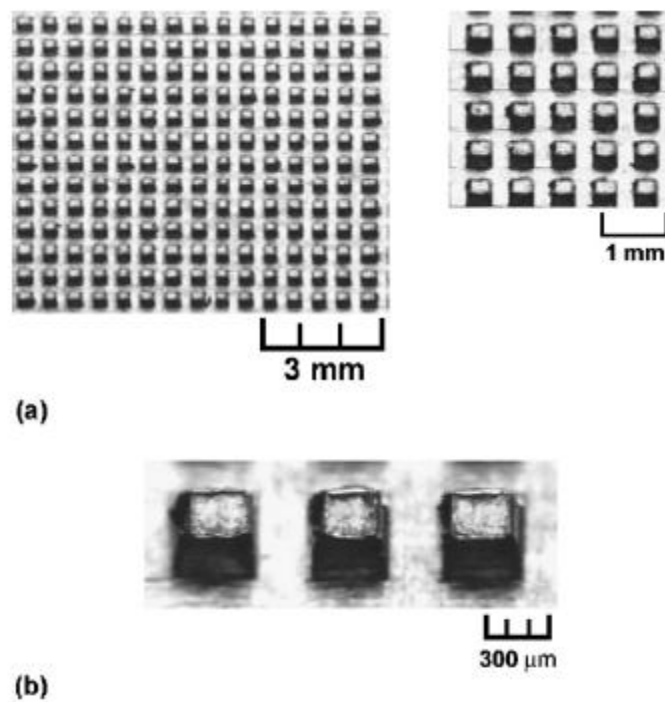


Figure 2.5: (a) Texture pattern of the substrate and (b) magnified view of the asperities (Katagiri et al, 2005)

From the experiments that were conducted, they concluded that on structured rough substrates textured substrates, an impacting liquid drop spreads simultaneously both inside the grooves and above the texture pattern of the substrate. For the impact of high-We drops, the liquid flowing inside the grooves of the textured substrate jet spreading dominates the spreading process. The spreading diameter measured for the liquid volume flowing above the texture pattern of the substrate is smaller than that on the smooth surface, mainly attributable to the decrease in the liquid kinetic energy available above the texture pattern.

In 1987, Timmons had studied the effect of sulfur-based encapsulants for fertilizers using modified sulfur, namely; dodecyl polysulfide (DDPS), carboxyethyl polysulfide (CEPS), and butoxycarbonyl polysulfide (BCEPS). He also conducted a study on the contact angle of liquid-sulfur on the surface of urea together with other polysulfides. The results of his discovery are summarized in Table 2.2. He mentioned that the contact angle affects the adhesive and cohesive strength of the sulfur coating.

Sulfur plus additive	Surface tension at T=125°C (dynes/cm)	Interfacial tension on urea at T=84°C (dynes/cm)	Contact angle on granular urea
Sulfur only	58	39.1	70°
2% DDPS	44	24.8	39°
1% CEPS	52	24.9	49°
1% BCEPS	52	55	55°

Table 2.2: Properties of sulfur-based encapsulants on urea (Timmons, 1987)

According to Link and Schlunder (1997), successful collision between a droplet of the liquid to be granulated and a seed particle is the fundamental step of coating and granulation process to determine whether a particle grows or otherwise. Particle growth through surface layering results in slow growth process creating rounded and uniformed granules with onion skin layered structure. Agglomeration is prevented by drying the wetted particle before collision with another droplet. Figure 2.6(a) shows the mechanism which leads to formation of new particles while Figure 2.6(b) shows the mechanism which leads to growth of particle.

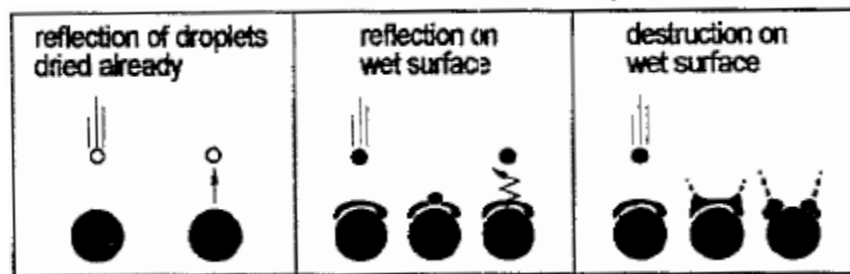


Figure 2.6(a): Mechanisms leading to formation of new particle (Link and Schlunder, 1997)

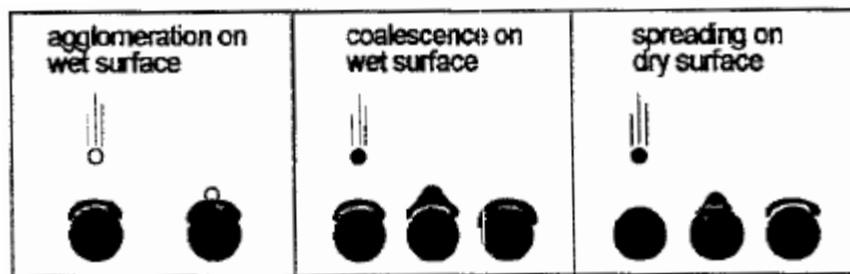


Figure 2.6(b): Mechanisms leading to particle growth (Link and Schlunder, 1997)

The velocity and size of both the droplet and collector particle influenced the impact of droplets on collector particles. Other factors include shape and density. Link and Schlunder (1997) pointed out that whether the droplet bounces or is captured, it depends on the interaction between droplet and particle surface. However, it needs to be noted that the probability of adhesion is not only a function of droplet momentum and physical properties of liquid, but also the function of surface characteristics of droplet and particle in the moment of collision.

According to Figure 2.6(a), new particles are formed when the sprayed droplets dry sufficiently prior to contact with the fluidized bed particles or when the moisture content is too high causing droplet reflection and destruction as proposed by Uhlemann. Agglomeration of dried droplets on wetted particles, coalescence of droplets on wetted surfaces and spreading on dry particles surfaces leads to particle growth (Link and Schlunder, 1997). The term wettability is used to describe the ability of droplet to wet the particle and spread on the surface. While spreading and coalescence causes the formation of uniformed and well-rounded granules, agglomeration of largely dried droplets leads to formation of raspberry type structures.

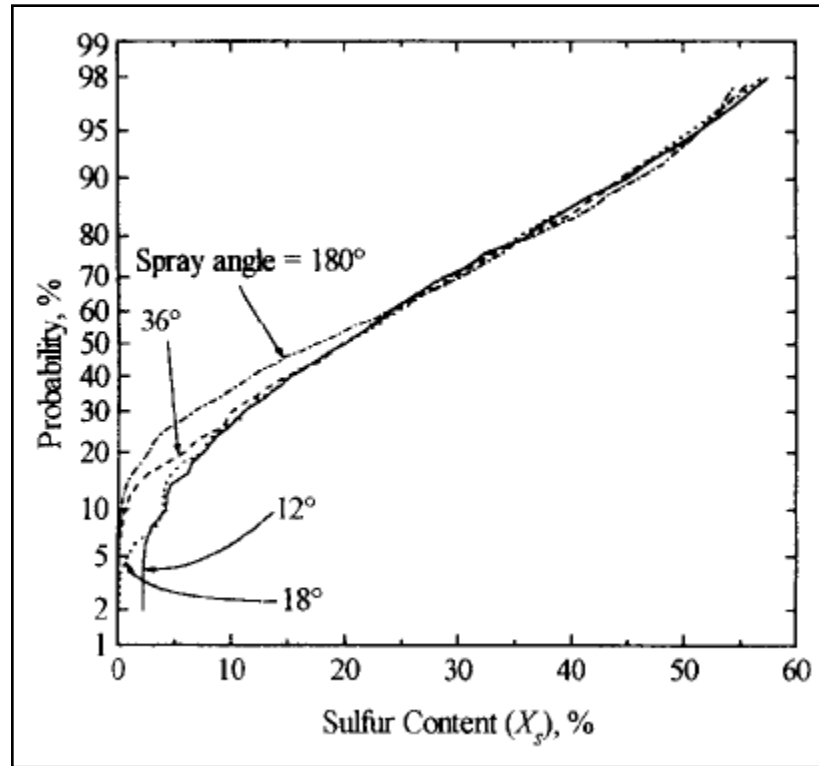


Figure 2.7: Effect of spray angle on coating distribution (Choi and Meisen, 1996)

Choi and Meisen (1996) stated that decreasing the spray angle in the spouted bed reduces the fraction of uncoated particles where the probability of sulfur content in coating the urea is reduced as spray angle is increased and vice versa. This is because the size of spray zone is reduced as the spray angle increases and in turn, leaves more particles uncoated. In their report, the urea which was coated at a spray angle of 180° has higher sulfur dissolution rate of seven (7) days as compared to those with a lower contact angle. Therefore, not only that the coating process of urea is affected by its surface roughness as well as the velocity of the sulfur droplet, but also by the spray angle of nozzle in the spouted bed unit.

2.3 Droplet Spreading Behavior: Simulation Approach

Ku Shaari (2007) has investigated the coating uniformity on a pharmaceutical tablet via experiment as well as simulation using Computational Fluid Dynamics (CFD) modeling software, Fluent®. The spreading of water droplet on pharmaceutical tablet surface is investigated. To do this, etched silicon surface, stainless steel, and tablets surface were used. The droplet size used was 2 mm. As for the modeling, a 3-D simulation was used to study the effect of contact angle, water surface tension, and surface roughness on the droplet spreading behavior. The results showed that as contact angle decreases from 90° to 45°, droplet tends to spread faster due to the fact that lower contact angle has lower surface energy which is governed by the Young's equation (Ku Shaari, 2007).

It is also noted that in the report, droplet with high contact angle has lower spreading diameter and less energy dissipation at the surface. The droplets retract and as the energy is transformed into kinetic energy, the droplet bounces upward faster and higher compared to those with lower contact angle.

Ku Shaari (2007) also performed studies on the effect of surface roughness on the spreading behavior of a droplet on flat surfaces with different roughness at ambient temperature. A static contact angle of 65° is used together with velocity of 0.5m/s on 'fine', 'smooth', 'rough' and 'very rough' surface. The results showed that droplet spreading diameter decreases as surface becomes rougher. This is because the friction on a smooth surface which has less energy dissipation assists in retaining the kinetic energy of the droplet, causing the droplet to continue spreading. The surface area with a 'very rough' surface generally has more surface area compared to that of a smooth surface. Figure 2.8 shows the spreading factor of droplets simulated on different surface roughness.

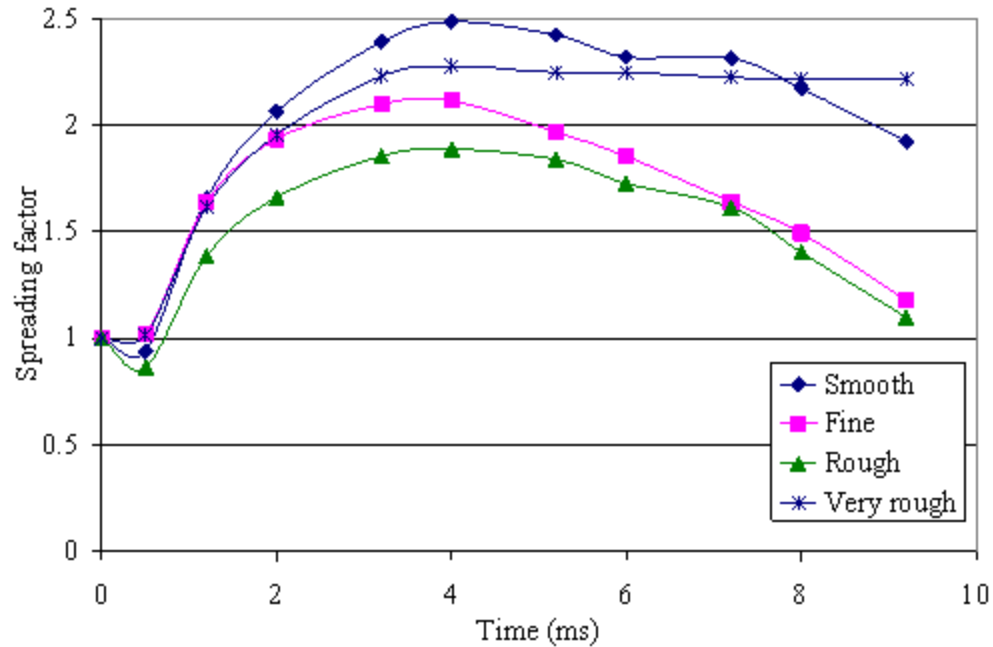


Figure 2.8: The spreading factor of the droplets simulated on different surface roughness (Ku Shaari, 2007)

Oukach et. al. (2010) has investigated deformation behavior of a liquid droplet impacting a solid surface by using COMSOL multiphysics for the simulation. Water droplet with a diameter of 3mm is used and a contact angle of 120° is chosen with velocity = 1.18m/s in 2D and 3D simulations. Before impact, droplet has a spherical shape and upon impingement, it starts to spread where a thin film forms at the solid surface. As the diameter increases, the thickness of the droplet decreases as can be seen in Figure 2.9. At $t = 4.7$ ms, the droplet reaches its maximum spread and a raised rim is formed at the margin of the lamella due to the increase of the mass by the surface tension forces which thwart the spread and decelerate the motion of the splat at the margin.

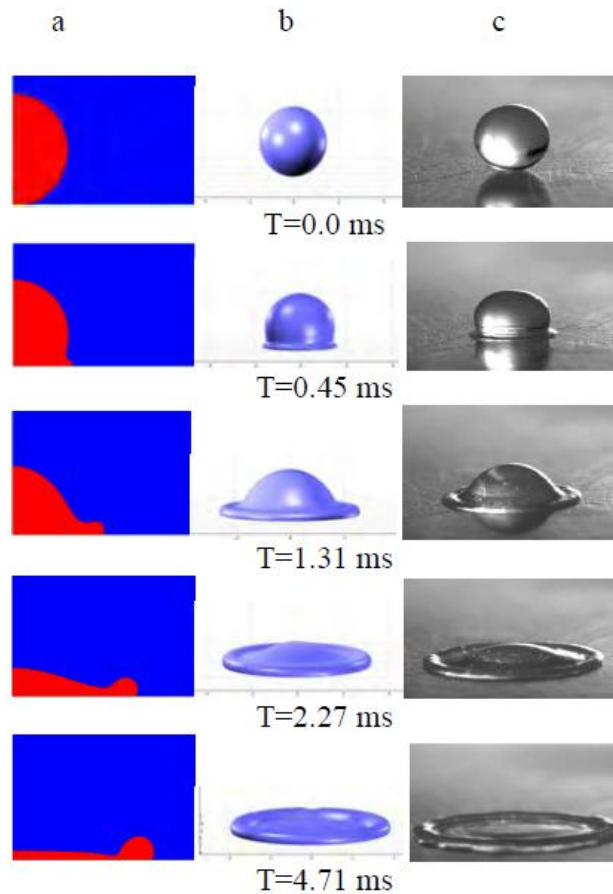


Figure 2.9: Impact and flattening of a 3 mm water droplet with a velocity $V_0 = 1.18$ m/s, (a) 2D simulation, (b) 3D simulation and (c) experimental results carried out by R.Rioboo (Oukach et. al., 2010)

Oukach et. al (2010) also reported that impact velocity has significant effect on droplet spreading where it produces significant changes in the shape of the splat. Increasing the impact velocity consequently increases spreading time as well as the spreading diameter of the droplet, and therefore, the spreading factor. At high impact velocity, it should be noted that phenomenon of splashing occurs as droplets are forced out from the rim of the lamella at the end of flattening; in which kinetic energy exceeds the surface tension force. It was also observed that in his report, droplet readily recoils and retracts for the

surfaces with high contact angle and lower velocity. When system is less wetted, the splashing occurs early; i.e., splashing occurs at 50m/s for contact angle of 120° and at 60 m/s when contact angle is 10° .

Much work has been done to predict the droplet spreading behavior on rough surface via experiment as well as simulation. However, CFD approaches to model the droplet spreading behavior on different surface roughness particularly that of a urea particle is still noticeably missing. The work has concentrated on establishing different types of coating material and effect of process conditions on particle growth for spouted bed coating of urea. For example, Liu et al (2007) used DCPD modified sulfur for urea particle coating and Rosa and Rocha (2010) analyzed the influences of operational variables on particle growth for urea coating in a conventional spouted bed similarly with Ayub et al (2001).

CHAPTER 3

METHODOLOGY

3.0 MODELING

Computational fluid dynamics (CFD) enables the study of the dynamics of things that flow. It allows the simulation flows of gases and liquids, heat and mass transfer, moving bodies, multiphase physics, chemical reaction, fluid-structure interaction and acoustics through computer modeling. A virtual prototype of the system or device can be built through this software to be analyzed and then apply real-world physics and chemistry to the model, and the software will provide images and data, which predict the performance of that design. Detailed flow diagram of activities is provided in Figure 3.1.

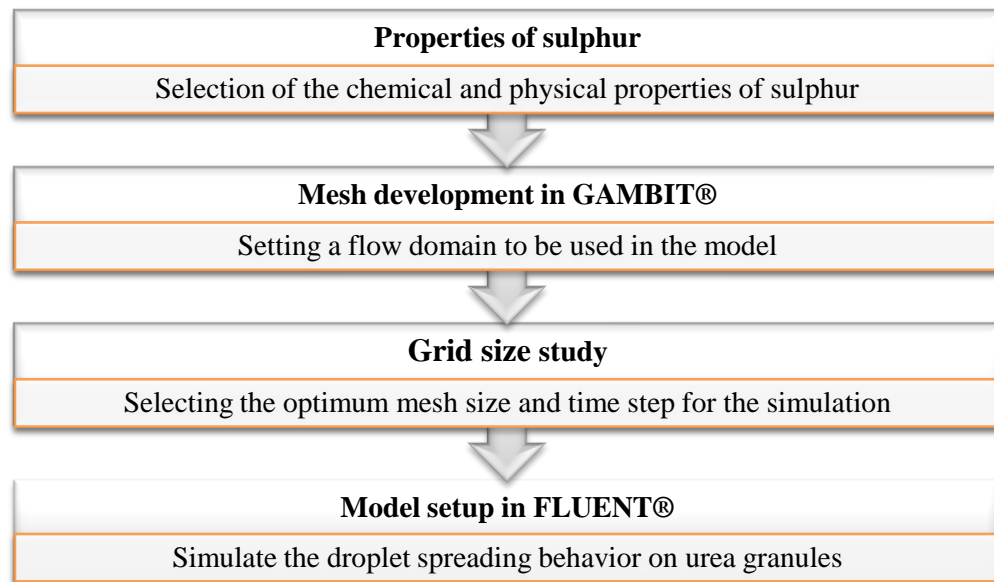


Figure 3.1: Project activities flowchart

Fluent software version 6.3.12 will be used to model the spreading of sulfur droplet in urea coating process. The GAMBIT® graphical user interface will be used to create mesh and geometries. The simulation will be performed in a computer with an Intel® Core™ 2 Duo processor and 2.00 GB RAM.

This chapter discusses the theory of multi-phase model used in this model called the volume of fluid (VOF). The development of the model will include the meshing technique to create a rough surface on the boundary wall condition and the surface tracking method used by VOF.

3.1 Volume of Fluid

The fields for all variables and properties are shared by the phases and represent volume-averaged values, as long as the volume fraction of each of the phases is known at each location. If the q th fluid's volume fraction in the cell is denoted as α_q , then the following three conditions are possible (©FLUENT Inc., 2003):

- (1) $\alpha_q = 0$: the cell is empty (of the q th fluid)
- (2) $\alpha_q = 1$: the cell is full (of the q th fluid)
- (3) $0 < \alpha_q < 1$: the cell contains the interface between the q th fluid and one or more other fluids.

Phases are treated as single fluid with material properties changing across the interface. Hence, each cell contains either a single face or an interface.

3.1.1 The Volume Fraction Equation

The volume fraction equation will not be solved for the primary phase; the primary-phase volume fraction will be computed based on the following constraint:

$$\sum_{q=1}^n \alpha_q = 1 \quad [3.1]$$

In a two-phase system, for example, if the phases are represented by the subscripts 1 and 2, and if the volume fraction of the second of these is being tracked, the density in each cell is given by:

$$\rho = \alpha_2 \rho_2 + (1 - \alpha_2) \rho_1 \quad [3.2]$$

Throughout the domain, only a single momentum equation is solved and the resulting velocity field is shared among the phases. The momentum equation (4.3) is dependent on the volume fractions of all phases through the properties ρ and μ .

$$\frac{\partial}{\partial t}(\rho \vec{v}) + \nabla \cdot (\rho \vec{v} \vec{v}) = -\nabla p + \nabla \cdot [\mu (\nabla \vec{v} + \nabla \vec{v}^T)] + \rho \vec{g} + \vec{F} \quad [3.3]$$

The energy equation, also shared among the phases is shown below:

$$\frac{\partial}{\partial t}(\rho E) + \nabla \cdot (\vec{v}(\rho E + p)) = \nabla \cdot (k_{\text{eff}} \nabla T) + S_h \quad [3.4]$$

Where the energy, E , and temperature, T , are treated as mass-averaged variables

$$E = \frac{\sum_{q=1}^n \alpha_q \rho_q E_q}{\sum_{q=1}^n \alpha_q \rho_q} \quad [3.5]$$

Where E_q for each phase is based on the specific heat of that phase and the shared temperature. The properties ρ and k_{eff} (effective thermal conductivity) are shared by the phases. The source term, Sh , contains contributions from radiation, as well as any other volumetric heat sources.

3.1.2 Surface Tension

Surface tension arises as a result of attractive forces between molecules in a fluid. The addition of surface tension to the VOF calculation results in a source term in the momentum equation. The importance of surface tension effects is determined based on the value of two dimensionless quantities: the Reynolds number, Re , and the capillary number, Ca ; or the Reynolds number, Re , and the Weber number, We . For $Re \ll 1$, the quantity of interest is the capillary number:

$$Ca = \frac{\mu U}{\sigma} \quad [3.6]$$

and for $Re \gg 1$, the quantity of interest is the Weber number:

$$We = \frac{\rho L U^2}{\sigma} \quad [3.7]$$

where U is the free-stream velocity. Surface tension effects can be neglected if $Ca \gg 1$ or $We \gg 1$.

3.1.3 Wall Adhesion

The contact angle that the fluid is assumed to make with the wall is used to adjust the surface normal in cells near the wall. This dynamic boundary condition results in the adjustment of the curvature of the surface near the wall.

If θ_w is the contact angle at the wall, then the surface normal at the live cell next to the wall is:

$$\hat{n} = \hat{n}_w \cos \theta_w + \hat{t}_w \sin \theta_w \quad [3.8]$$

Where \hat{n}_w and \hat{t}_w are the unit vectors normal and tangential to the wall. The combination of this contact angle with the normally calculated surface normal one cell away from the wall determine the local curvature of the surface, and this curvature is used to adjust the body force term in the surface tension calculation. Figure 3.2 illustrates the measurement of contact angle.

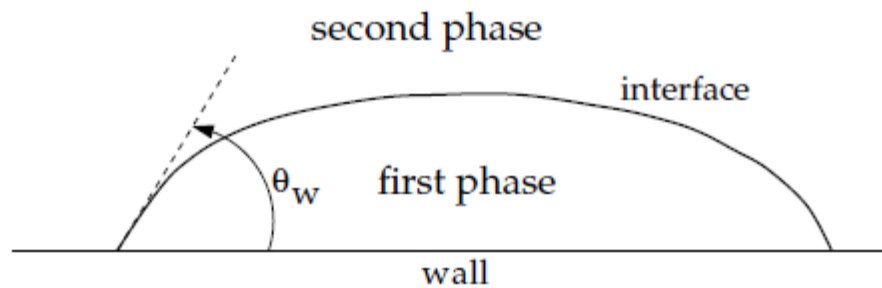


Figure 3.2: Schematic diagram of the contact angle between phases (Fluent Inc.© 2003)

3.2 Gantt Chart

In order to ensure timely completion of project the progress will be tracked using the Gantt chart in Table 3.1 and Table 3.2:

Activities	August	September	October	November
Selection of FYP topic	■			
Submission of Proposal (06/08/2010)	■			
Preliminary Research Work		■		
Submission of Progress Report (03/09/2010)		■		
Seminar 1 (03/09/2010)		■		
Project Work		■	■	
Seminar 2				■
Submission of Interim Report (04/11/2010)				■
Oral Presentation (02/11/2010)				■

Table 3.1: Project Gantt chart (Final Year Project 1)

Activities	May	June	July	August
Project Work continues		■	■	
Submission of Progress Report (Week 8)			■	
Project Work Continues			■	■
Pre-EDX (Week 11)				■
Submission of Draft Report (Week 12)				■
Submission of Dissertation (soft bound)				■
Submission of Technical Paper				■
Oral Presentation				■
Submission of Project Dissertation (hard bound)				■

Table 3.2: Project Gantt Chart (Final Year Project 2)

3.3 Key Milestone

For the objectives of this project to be accomplished, there are several milestones needed to be achieved as shown in Table 3.3:

1. Mesh development in GAMBIT to be used in the model	Oct 2010
2. Simulate droplet spreading behavior on smooth surface	Nov 2010
3. Obtain Scanning Electron Microscopy (SEM) images of urea	Dec 2010
4. Grid size study for optimum mesh size and time step size	May 2011
5. Simulate droplet spreading behavior on the surface of urea	June 2011
6. Study the effect of velocity impact of droplet spreading on the surface of urea	June 2011
7. Study the effect of contact angle of droplet spreading on the surface of urea	July 2011
8. Submission of Dissertation	September 2011

Table 3.3: Key Milestone of Project

CHAPTER 4

PROJECT WORK

4.0 SIMULATION

4.1 Grid Size Study

Before determining the optimum mesh size and time step size for running the simulation, grid size study needs to be done. The purpose of the grid size study is not only for the simulation to run smoothly but it also saves time as well as cost while doing the project. Table 4.1 and Table 4.2 summarize the grid size and time step size which were used to enhance the simulation.

Mesh size (mm)
0.02
0.025
0.035
0.05
0.055
0.06
0.065
0.07

Table 4.1: Grid size used for the grid size study

Time step size (s)
1×10^{-05}
1×10^{-06}
1×10^{-07}
1×10^{-08}

Table 4.2: Time step size used for the grid size study

For each of time step size, different mesh size is used to obtain a graph of y-velocity versus time step size. The results are then computed and the graph which shows no change or is independent of the grid size is selected. For this project, the most appropriate mesh size is 0.025mm x 0.025mm with a time step size of 1.0×10^{-07} second. The graph for this grid size study is further discussed in the results section under Chapter 5.

4.2 Mesh Development in Gambit®

A domain has to be developed to the flow system before the dynamics of flow can be simulated. In this project, Gambit® software was used to generate a geometry and grid of the flow domain used in the model. The dimensions of the geometry are 2mm X 8mm illustrated in Figure 4.1. The grid size or more properly known as mesh was set to 0.025 mm x 0.025 mm.

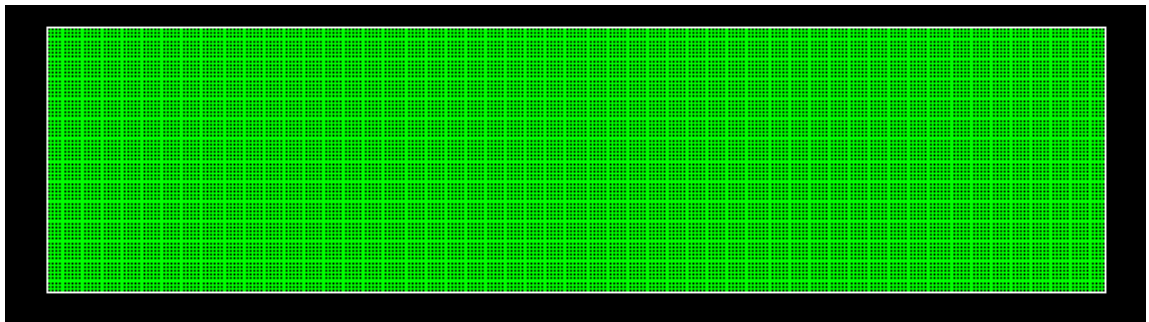
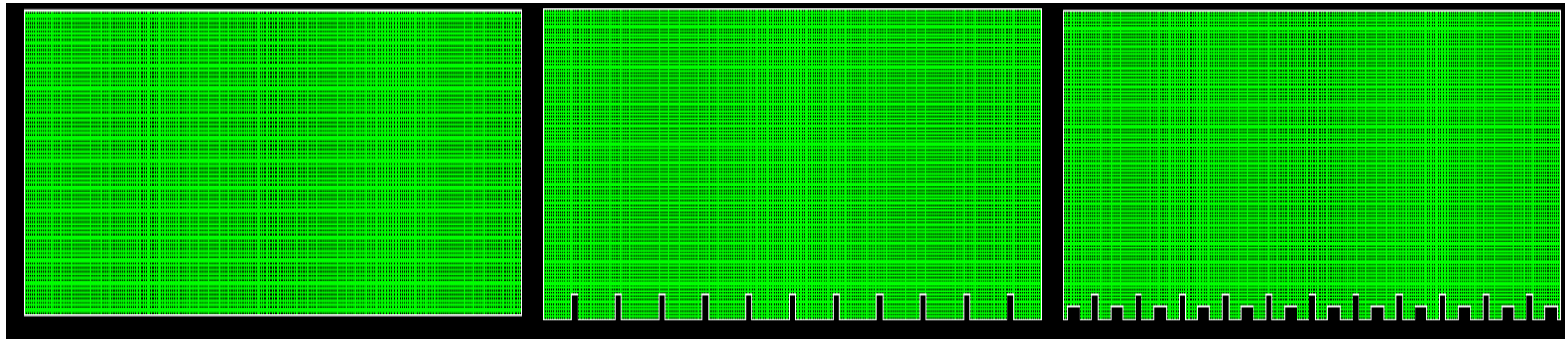
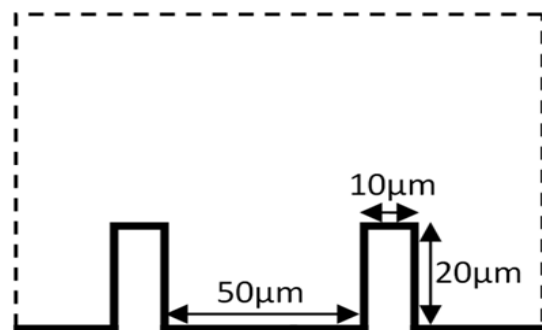


Figure 4.1: Flow domain used in the model with length (x-axis) and width (y-axis) equal to 8 mm and 2 mm, respectively

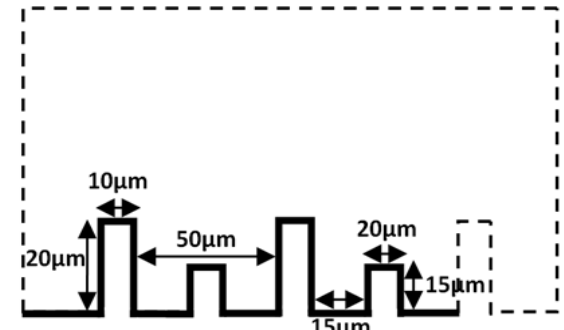
Similar domain was created as well; however, rough surface was structured along the y-axis to simulate the roughness of the urea. This is then used to study the effect of the rough surface towards the spreading behavior of the sulfur droplet. Two models of rough surface were generated and the parameters are shown in Figure 4.3 and Figure 4.4. Figure 4.2 summarizes the images of the meshed flow domain for the three different types of surfaces; smooth, rough, and very rough.



Smooth surface



Rough surface



Very rough surface

Figure 4.2: Side view image of the meshed flow domain the three different types of surfaces; smooth, rough, and very rough with schematic diagram of dimensions for the rough pattern

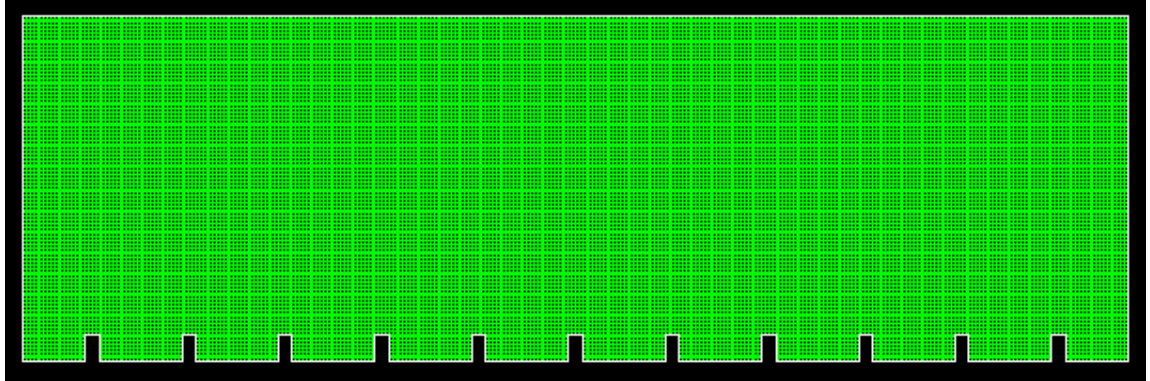


Figure 4.3: Flow domain of “rough” surface

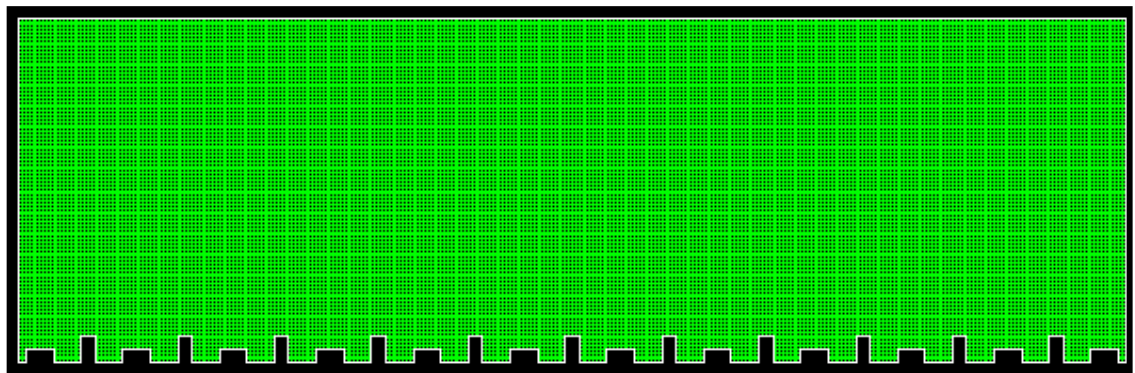


Figure 4.4: Flow domain of “very rough” surface

As can be seen in Figure 4.3 and Figure 4.4, the very rough surface was structured with horizontal rectangles in between the present vertical rectangles which were structured for the rough surface. This is because on the surface of a urea, SEM images have shown that the surface roughness of a urea is not uniform. The SEM images of the urea can be found in Chapter 5 under results section.

4.3 Assumptions and Physical Model Set-up

Several assumptions are undertaken while using the model:

1. The ambient air is stagnant.
2. The liquid droplet is spherical at the time of impact.
3. The liquid is incompressible with constant surface tension and viscosity.
4. Newtonian and laminar fluid.
5. No-slip boundary condition along the solid surface with no penetration.
6. The boundary condition does not include evaporation.

In the model, two phases are specified; phase 1 and phase 2. Phase 1 is defined as air while phase 2 is defined as sulfur-liquid. Phase 1 has to be compressible gas to improve solution solubility.

The model in this work requires a time-dependent solution, an explicit scheme from the VOF formulation was applied to the volume fraction values:

$$\alpha_{qq}^{i+1} + \rho_q^{i+1} + \sum_f (\rho_q J_f^i \alpha_{q,f}^i) = [\sum_{p=1}^i (\dot{m}_{pq} - \dot{m}_{qp}) + S_{\alpha q}] V \quad [4.1]$$

Where $i+1$ is the new time step, i is the previous time step, α_{qf} is the face value of the q^{th} volume fraction, V is the volume of cell and J_f is the volume flux through the face, based on normal velocity.

From this scheme, the time step size can be determined. To ensure that the fluid uses up enough time in a cell, selecting the time step size is important to assist in convergence. The time step size for the volume fraction calculation depends on the maximum Courant number, Co which is defined by:

$$Co = \frac{\Delta t}{\Delta x/v} \quad [4.2]$$

Where Δt is the time step size, Δx is the size of a cell in the x-direction, and v is the fluid velocity or the impact velocity. The Courant number is set to 0.25 by default. For the volume fraction, the resulting time step is the time taken by the fluid to empty the cell.

4.4 Factors affecting droplet spreading behavior

To study the spreading behavior of sulfur droplet on the surface, several parameters needed to be taken into consideration as well such as the physical properties of molten sulfur, the velocity impact, and the contact angle. The physical properties of the molten sulfur at different temperature can be found in Table 4.2.

Temperature (°C)	130	140	150
Density (kg/m³)	1795.7	1787.0	1778.4
Viscosity (poise)	0.092	0.077	0.075
Surface tension (dyne/cm)	59.83	58.77	57.70

Table 4.3: Physical properties of molten sulfur at different temperatures

In this project as well, the impact of different velocity of the droplet towards its spreading behavior would be taken into consideration together with the effect of different contact angle on the spreading of sulfur droplet. Table 4.3 shows the different velocity and contact angle which is used to study the effect on the spreading behavior.

Velocity impact (m/s)	Contact angle
-0.5	30°
-1.5	60°
-3	120°

Table 4.4: Velocity impact and contact angle of molten sulfur

4.5 Solution Initialization and Iteration

The volume fraction for phase 2, which is the molten sulfur droplet, is assigned to a value of 1. The impact velocity of -0.5 m/s was also specified. For the groundwork of this project, molten sulfur properties at 150°C will be used as this temperature of molten sulfur is widely used in the production of sulfur coated urea in the fertilizer industry. These parameters are summarized in Table 4.4.

Impact velocity	-0.5 m/s
Contact angle	120°
Density_{@150°C}	1778.4 kg/m ³
Viscosity_{@150°C}	0.075 poise
Surface tension_{@150°C}	57.70 dyne/cm

Table 4.5: Sulfur droplet specifications

Once the material has been selected and set, liquid sulfur will be patched into the flow domain that was created earlier. Figure 4.4 shows the initial form of the flow domain after the spherical region has been patched into the domain of smooth surface using Fluent®. Non iterative time advancement scheme is used during the iteration to reduce computational time.

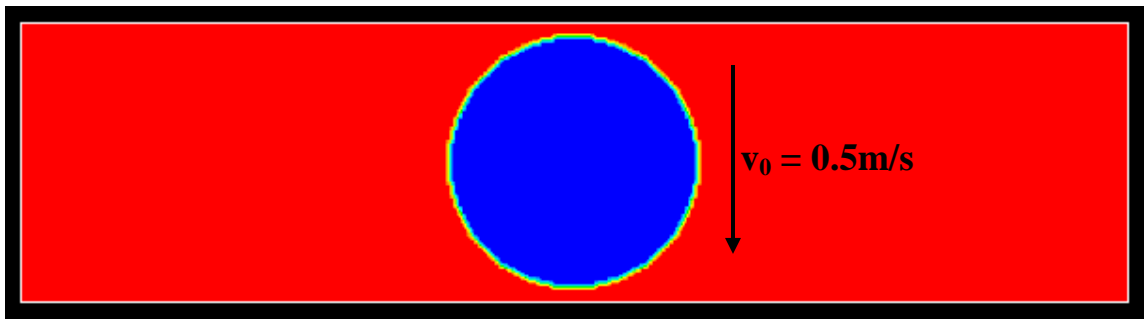


Figure 4.5: Initial condition of the flow domain after phase 2 (sulfur-liquid) was patched into the system

CHAPTER 5

RESULTS AND DISCUSSION

Imperfection of the coating layer during the prilling or the rotary drum coating process often leads to an opening on the sulfur-coated urea particle (Weiss and Meisen, 1983). The sulfur-coating layer is not permeable to water; hence, urea is only released at the opening to the surrounding (Doan et al, 1999). This shows that the uneven surface of the urea particle affects the droplet behavior, giving an irregular coating of sulfur. Figure 5.1 shows the comparison between uncoated urea particles and sulfur-coated urea particles.

While Figure 5.1 shows the images of uncoated urea by Ayub et. al. (2000), Figure 5.2 shows the image of urea formaldehyde taken using Scanning Electron Microscopy (SEM) at magnification of 20X and 300X at room temperature. Comparatively, the urea images between Figure 5.1 and Figure 5.2 for the magnification of 20X as well as 300X are quite similar. At 20X, the urea's surface appears to be smooth, however, at higher magnification; it can be observed that certain surface area of the urea is smooth as shown in Figure 5.2(c) and certain surface area of the urea can be seen as rough as shown in Figure 5.2(d).

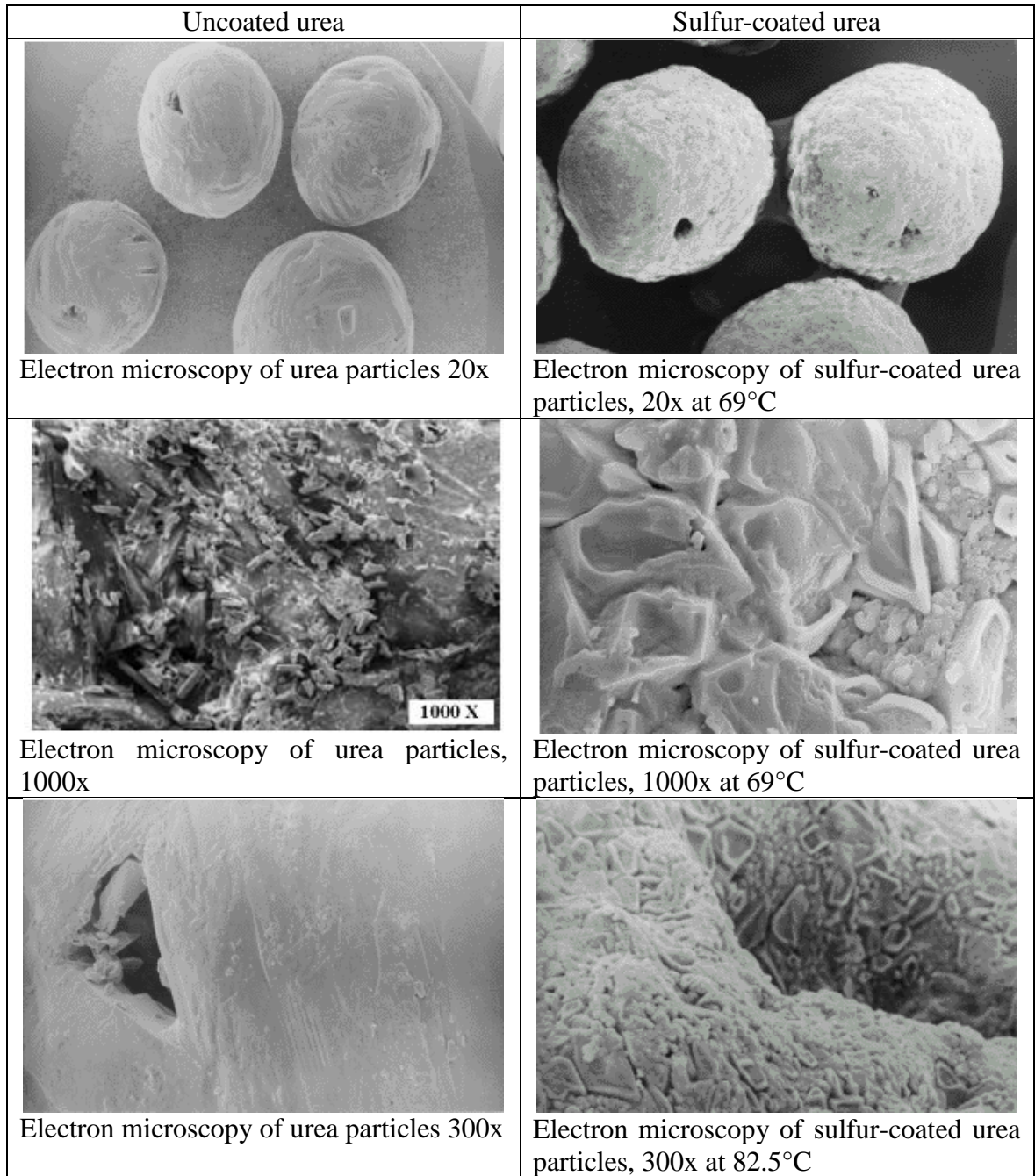
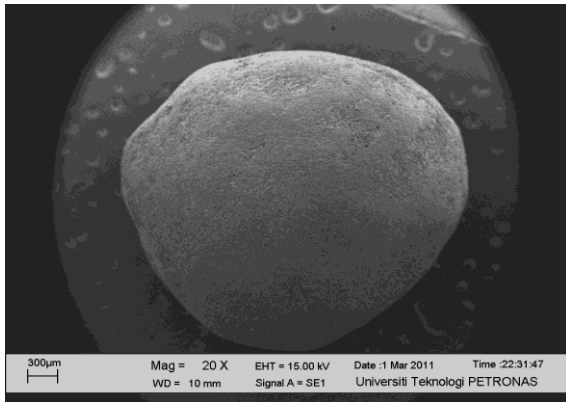
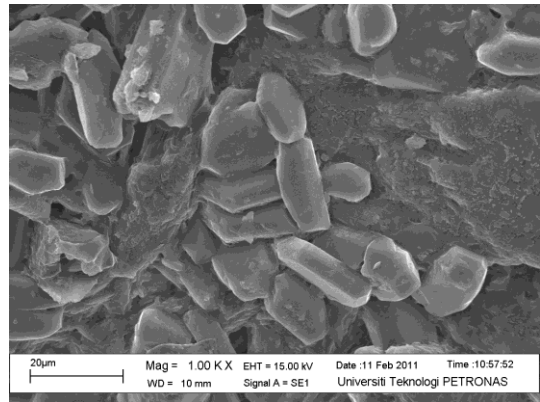


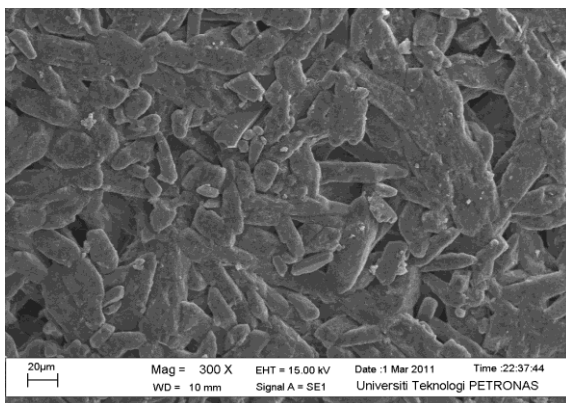
Figure 5.1: Electron microscopy of uncoated and coated urea particles (Ayub et al, 2000)



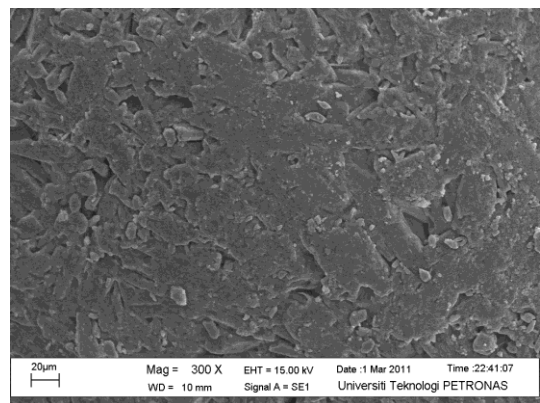
(a) SEM image of urea at 20X



(b) SEM image of urea at 1000X



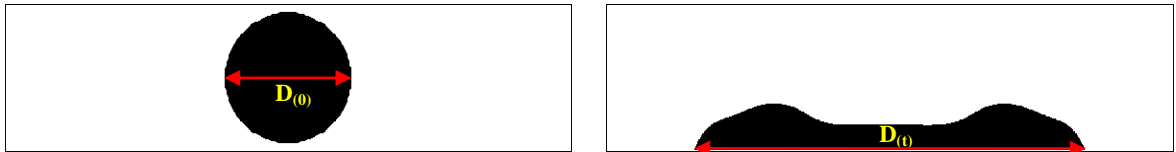
(c) SEM image of urea at 300X showing rough area of urea



(d) SEM image of urea at 300X showing smooth area of urea

Figure 5.2: SEM images of uncoated urea at 20X, 300X, and 100X

Besides the effect of surface roughness on spreading behavior of droplet, other factors such as contact angle and velocity impact would be investigated further throughout the duration of this project. To predict the maximum spreading diameter of a droplet, a model was developed using Computational Fluid Dynamics (CFD) software; Fluent® that predicts the initial spreading of a droplet on different surface roughness. The study of the initial spreading of a droplet provides important information on the maximum spreading diameter, which also gives the coating coverage resulting from the droplet impact. The spreading factor is illustrated in Figure 5.3 where it is defined as the ratio of the droplet on the surface at time t , to the initial droplet diameter at time t_0 .



$$\text{Spreading factor} = \frac{D(t)}{D(0)}$$

Figure 5.3: Definition of spreading factor (Ku Shaari, 2007)

5.1 Grid Size Study Results

As previously mentioned in the methodology section under Chapter 4, grid size study was done to determine the optimum grid size as well as the time step size for the simulation. It can be seen in Figure 5.4 that the results are similar from one grid size to another, hence, providing the fact that the grid size is independent of the time step size used.

The relationship between the grid size and the time step size is given by:

$$\Delta t = \frac{\Delta x}{V_f} \quad [5.1]$$

Where Δt is the time step size, Δx is the grid size measured in the x-direction, and V_f is the fluid velocity in the cell. The magnitude of the Δt should be estimated to result a small Δx than the grid size. Based on the maximum Courant number allowed near the free surface, Δt is then defined automatically.

Comparing this graph to Appendix 1 and Appendix 2, although time step size of 1×10^{-08} in Appendix 3 provides similar results, time step size of 1×10^{-07} is more time saving compared to that of 1×10^{-08} . The optimum grid size used for this simulation is 0.025mm x 0.025mm. After patching the spherical droplet shape onto the domain, it can be observed that in bigger mesh size, the edge of the spherical shape is uneven while on the grid size of 0.025mm, the edge is smooth and even.

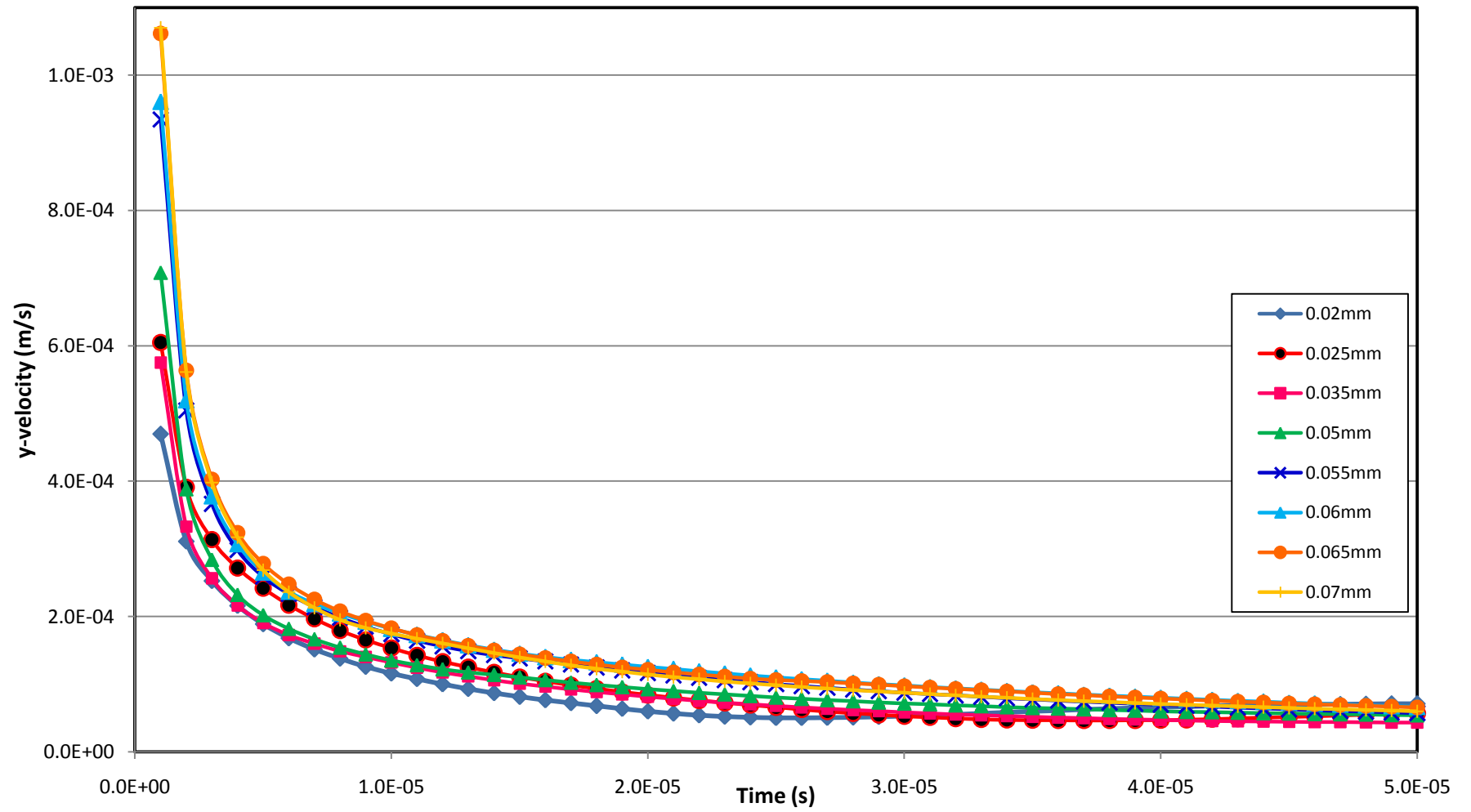


Figure 5.4: Grid size independent study of 1.8mm droplet on smooth surface at constant contact angle=120° and velocity=0.5m/s

5.2 Simulation Results

To simulate the initial impact behavior of liquid-sulfur, a volume of fluid (VOF) multiphase model was developed. A 2D model was used in this work due to its simplicity. The model was used to show the effect of different surface roughness, contact angle, and impact velocity on the spreading behavior of the droplet. The simulations were run using a uniform grid with a time step of 1×10^{-07} second. The wall adhesion term in the boundary condition panel was activated to enable the use of contact angle. The model was run in a 2-phase setting, with air as the main phase and sulfur-liquid as the secondary phase. Two different kinds of surface roughness were also developed and using the same parameters as the smooth surface, the spreading behavior of the droplet was also produced. This was further discussed in methodology section in Chapter 4.

5.2.1 Effect of different surface roughness

A 2D model was developed to study the effect of surface roughness in the simulation. Figure 5.4 shows the results of the simulation from the modeling of liquid-sulfur droplet spreading behavior on smooth surface as well as the rough surface with an impact velocity of 0.5 m/s, droplet diameter of 1.8 mm, and contact angle of 30° . It can be observed that spreading factor is higher on smooth surface; Figure 5.7(a) as compared to very rough surface in Figure 5.7(c). The droplet spreading diameter decreases as the surface becomes rougher and can be seen in Figure 5.6. This is because the rougher surface provides more surface area and promotes more friction, therefore slowing down the spreading (Ku Shaari, 2007).

As can be seen in Figure 5.7(b) and Figure 5.7(c), the droplets are sitting on small air pocket instead of penetrating entirely into the substrate. This can be explained using the Wenzel model. The rough surface is a heterogeneous surface unlike the homogenous surface of the smooth surface, where the advancing and receding of contact angles are

equal which has only one thermodynamically stable contact angle. For the Cassie-Baxter model, the droplet sits on top of the textured substrate trapping small air pockets underneath it. The Cassie-Baxter model is further discussed in Section 5.2.2 of this chapter. The air pockets are no longer thermodynamically stable during the wetting transition of Cassie-Baxter model to Wenzel model, therefore liquid begins to disintegrate from the middle of the drop, creating a “mushroom state,” which is illustrated in Figure 5.5.

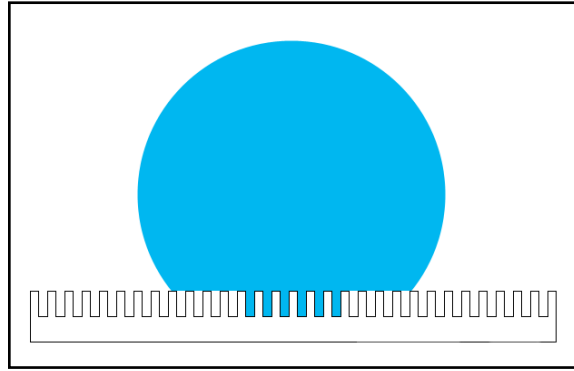


Figure 5.5: Mushroom state (Sanders, 2010)

The penetration is governed by Equation (5.2). The penetration front spreads to decrease the surface energy until it reaches the edges of the drop, thus arriving at the Wenzel state. This phenomenon of spreading and imbibition is called hemi-wicking since the solid can be considered a kind of porous material due to its surface roughness (Bico et. al., 2002). Spreading and imbibition occurs at the contact angles between $0 \leq \theta < 90$.

$$\cos \theta_c = \frac{1 - \phi_s}{r - \phi_s} \quad [5.2]$$

Where, θ_c is the critical contact angle, ϕ_s is the fraction of the solid-liquid interface below the drop, and r is the solid roughness (for flat surface, $r = 1$). The Wenzel model is valid between $\theta_c < \theta < 90$. If the contact angle is less than θ_c , the penetration front spreads beyond the drop and a liquid film forms over the surface, where the film smoothes the surface roughness of the Wenzel state.

As can be observed from Figure 5.6, the arrangement for the increasing surface area is;

Smooth < Rough < Very rough

where it is shown that smooth surface has the highest spreading factor, followed by rough surface and lastly, very rough surface.

However, it must be noted that from the SEM images that was taken, certain area of the urea appears to be smooth and certain area of the urea appears to be rough. Hence, it can be deduced that where the droplet would be in contact with the urea's surface in the spray coating bed will affect its spreading factor.

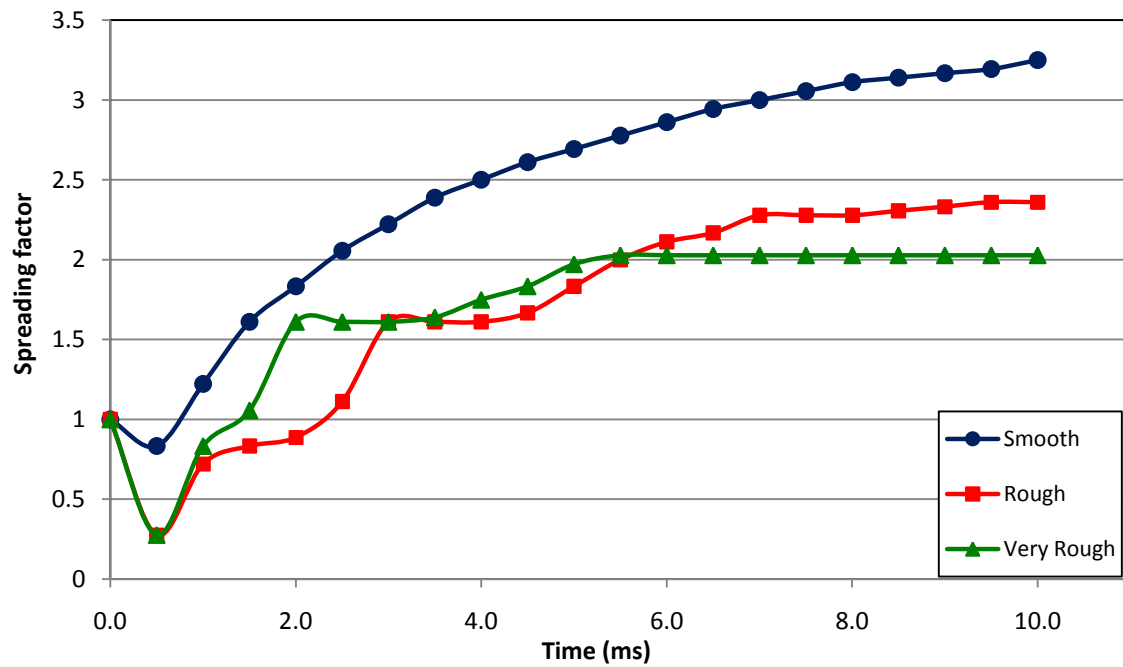


Figure 5.6: The droplet spreading behavior on different surface roughness

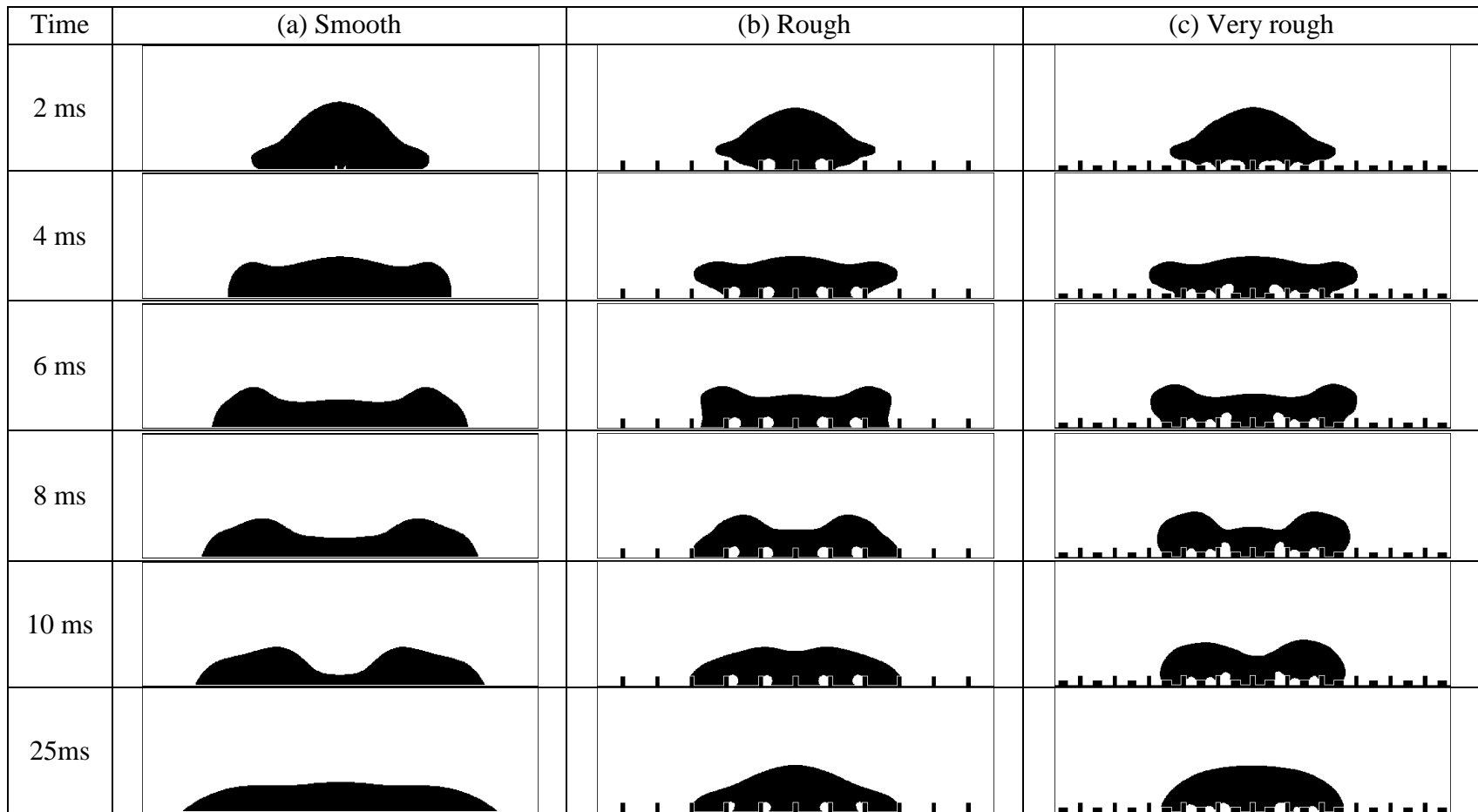


Figure 5.7: Computer generated images of the liquid droplet on different surface roughness

5.2.2 Effect of different contact angle

Contact angle plays a significant role in droplet spreading and can be defined as the angle at which a liquid/vapor interface meets a solid surface, as shown in Figure 5.8. Different pairs of liquids and solids have different contact angles that depend on the properties of the liquid and surface. There are two types of contact angle; dynamic contact angle and static contact angle. During spreading, the contact angle changes with time is called dynamic contact angle. When the droplet is at rest, the angle formed by the droplet on the surface is called static contact angle.

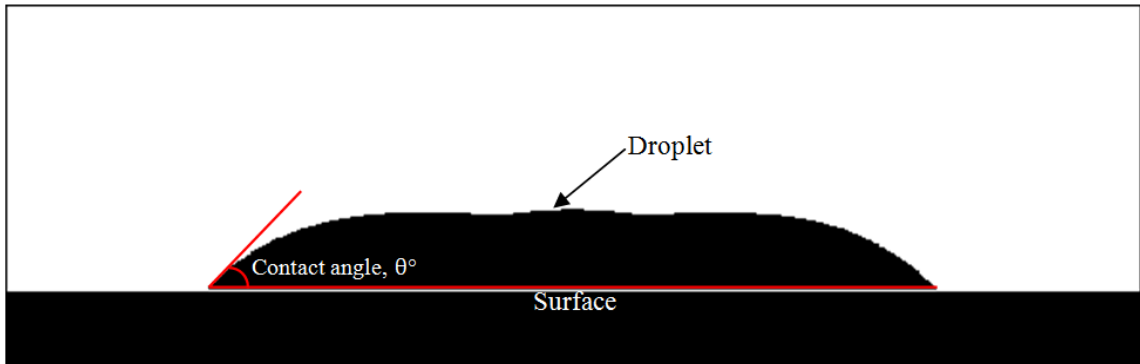


Figure 5.8: Measurement of contact angle

A number of simulations were run with different static contact angles specified at the wall boundary condition to investigate the effect of different static contact angles on the spreading behavior of droplet in the simulation. The simulations were conducted using the same grid and time step size and at the same impact velocity of 0.5m/s. Figure 5.12, 5.14, and Figure 5.15 shows the image comparison between different surface roughness at contact angles of 30°, 60°, and 120°, respectively.

Figure 5.9 shows that for lower contact angle, i.e. 30°, droplet tends to spread faster. This is because lower contact angle has lower surface energy indicating that wetting of the surface is favorable. As contact angle increases, the surface energy increases and less spreading occurs. This phenomenon can be explained by using Young's equation which is given by Equation (5.3).

$$\sigma_{LV} \cos \theta = \sigma_{SV} - \sigma_{SL} \quad [5.3]$$

Where σ_{LV} , σ_{SV} , and σ_{SL} are the liquid-vapor energy or surface tension, solid-vapor interfacial energy, and solid-liquid interfacial energy, respectively. The decrease of the spreading diameter of the droplet can be seen when $CA = 120^\circ$ as shown in Figure 5.9, Figure 5.10, and Figure 5.11 for smooth surface, rough surface, and very rough surface, respectively. The results also show that as contact angle increases ($CA = 120^\circ$), the droplet rebounds at 10ms for smooth surface. The droplet with high contact angle has lower spreading diameter and higher surface energy. In Ku Shaari's (2007) report of coating uniformity on a pharmaceutical table, water droplet with $CA = 60^\circ$ starts to recoil at $t = 8\text{ms}$ on rough stainless steel surface. With high contact angle, the droplet experience less energy dissipation at the surface (Ku Shaari, 2007).

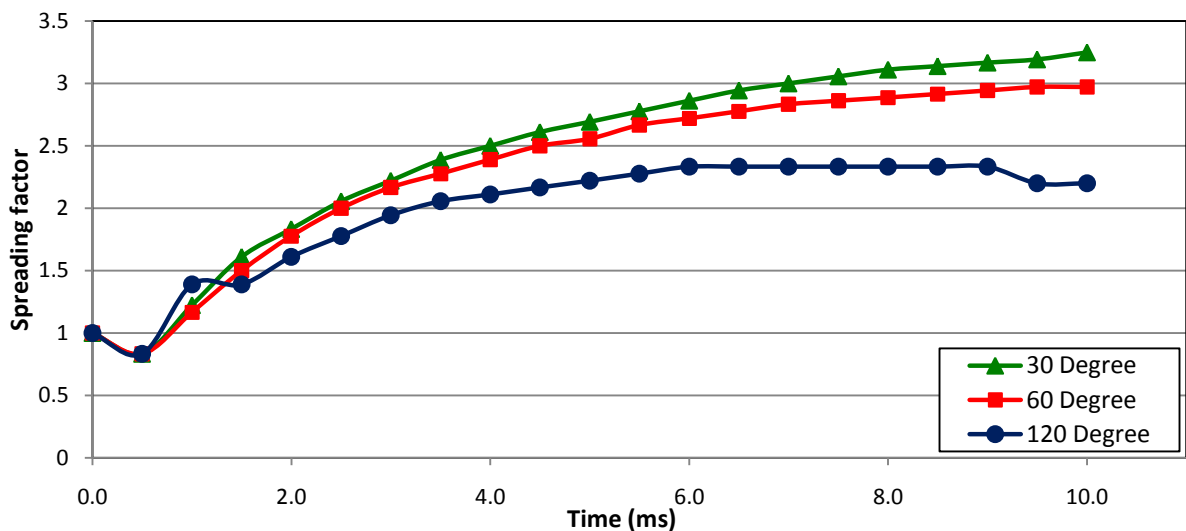


Figure 5.9: The spreading factor of droplet on 'smooth' surface

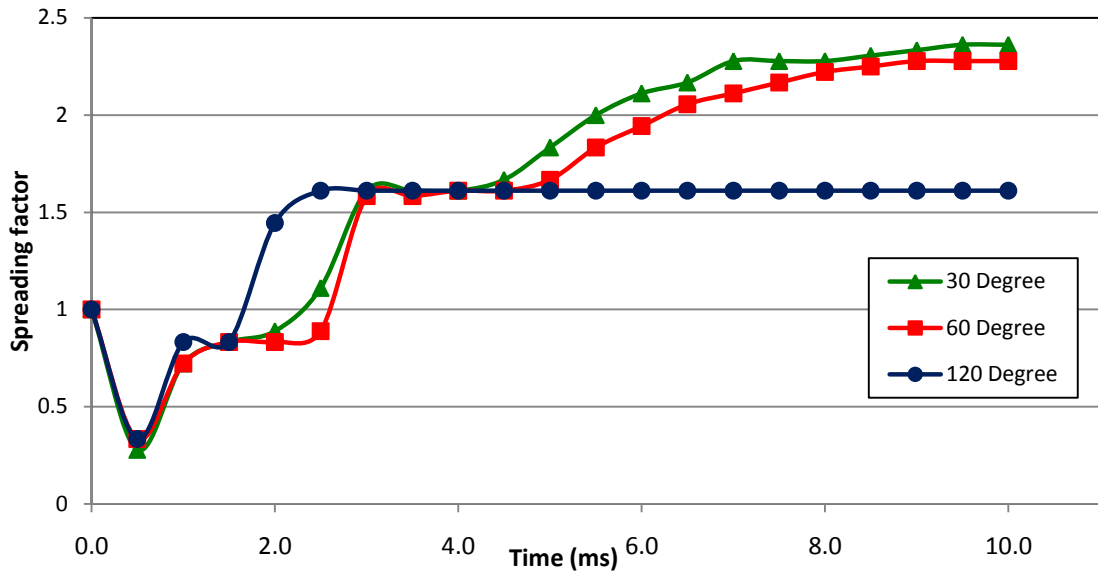


Figure 5.10: The spreading factor of droplet on 'rough' surface

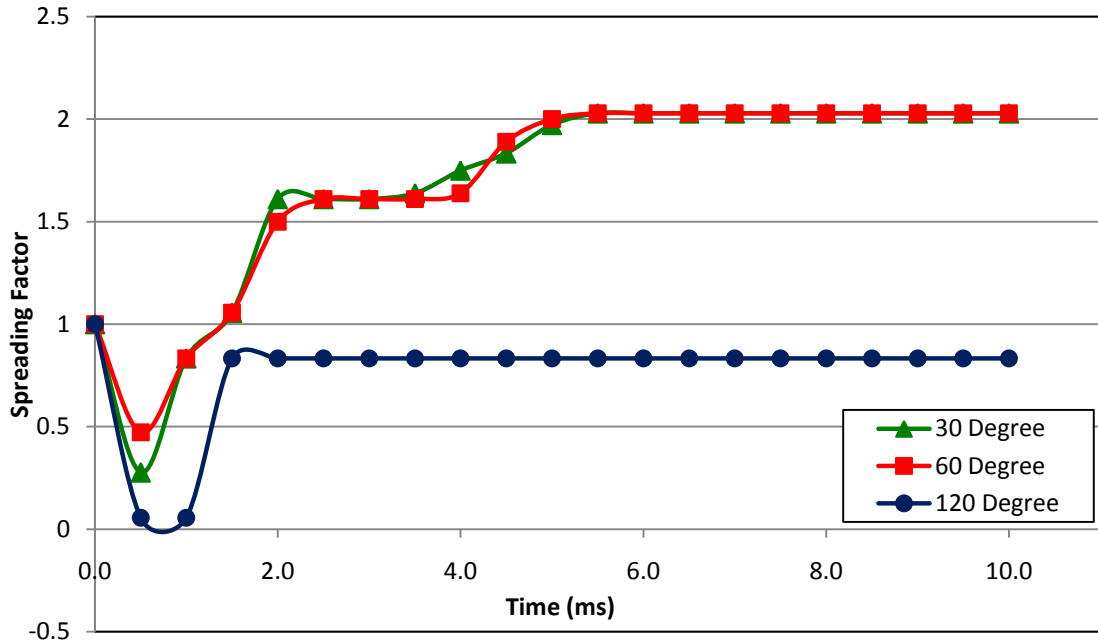


Figure 5.11: The spreading factor of droplet on 'very rough' surface













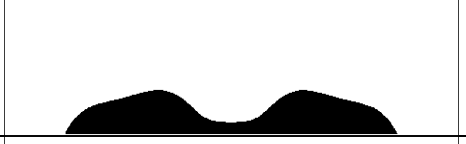





Time/Contact angle	(a) 30°	(b) 60°	(c) 120°
2 ms			
4 ms			
6 ms			
8 ms			
10 ms			
25ms			

Figure 5.12: Computer generated images of the liquid droplet on ‘smooth’ surface at different contact angle

As can be seen in Figure 5.14(c) of rough surface, at $CA = 120^\circ$, the droplet does not penetrate into the substrate. When the sulfur droplet impacted the substrate, it traps small air pockets underneath it. This phenomenon can also be similarly seen in Figure 5.15(b) of very rough surface at $CA = 60^\circ$. The heterogeneous surface can be explained using Cassie-Baxter's equation.

$$\gamma \cos \theta^* = \Phi (\gamma_{SV} - \gamma_{SL}) - (1 - \Phi)\gamma \quad [5.4]$$

Where $\gamma \cos \theta^*$ is the Cassie-Baxter apparent contact angle, Φ is the fraction in the substrate surface, $1 - \Phi$ is the air surface fraction under the droplet, and γ , γ_{SL} , and γ_{SV} are the surface tensions at the liquid-vapor, solid-liquid, and solid-vapor interfaces, respectively. Figure 5.13 shows the Cassie-Baxter regime where air is trapped under the droplet.

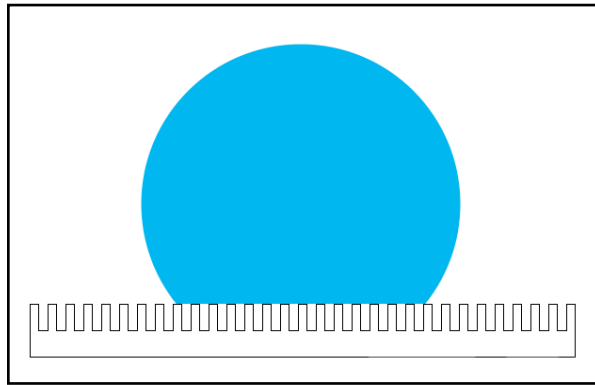


Figure 5.13: Rough substrate where air is trapped under the drop (Whyman et. al, 2007)

However, in actual spray coating process of the urea, the molten sulfur droplet does penetrate into the urea as urea is hydrophilic, where the Cassie-Baxter model transitions to the Wenzel model as previously discussed in Section 5.2.1.

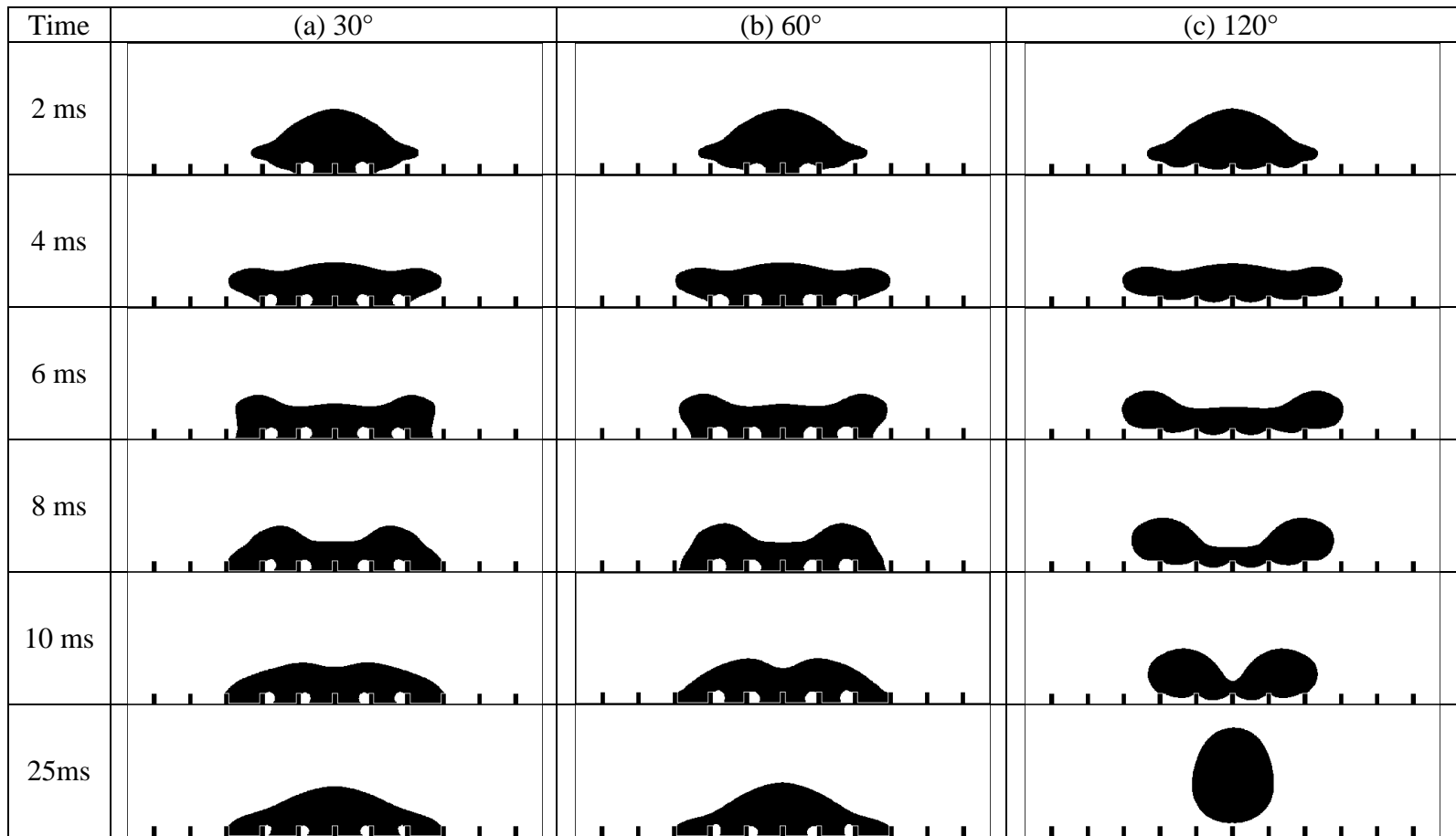


Figure 5.14: Computer generated images of the liquid droplet on 'rough' surface at different contact angle

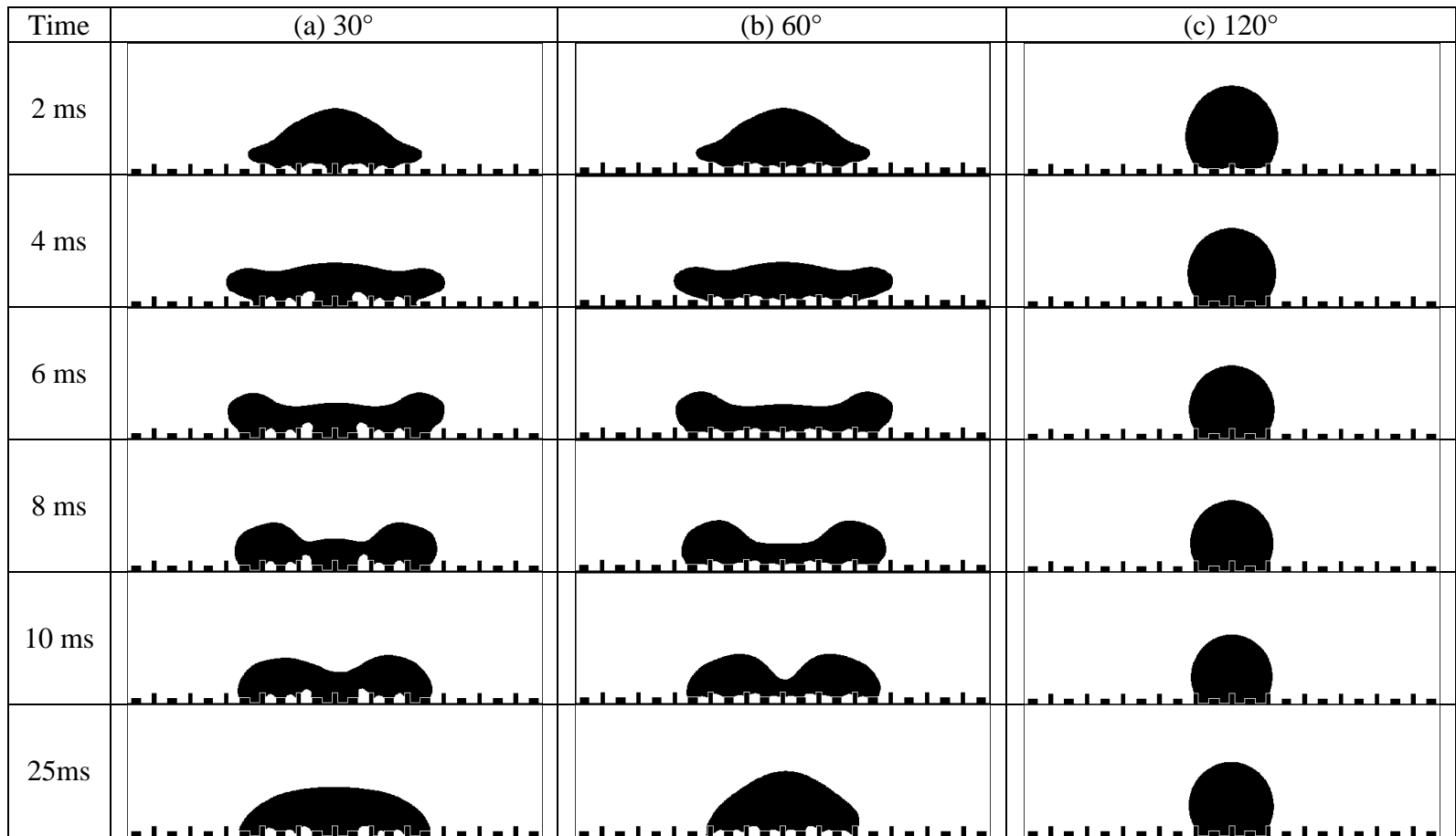


Figure 5.15: Computer generated images of the liquid droplet on 'very rough' surface at different contact angle

Zahirah (2011) investigates the surface tension and contact angle of biomass liquid; a mixture of urea, starch, and borate combined together either with cellulose, lignin, and clay. The combination of urea/starch/borate with 20% lignin concentration gives the closest result to that of a sulfur droplet by having the same surface tension which is between 56 – 58 dynes/cm. Figure 5.16 shows the experimental data that was obtained for that of the droplet with 20% lignin concentration. Based on the results obtained, contact angle of 30° from the simulation gives a better agreement with the experimental data. Table 5.1 summarizes the results that were obtained from the experiment.

Surface	Contact angle (θ°) of 20% Lignin
Glass	35° – 49°
Urea	20° – 35°

Table 5.1: Contact angle of 20% lignin on surface of glass and urea

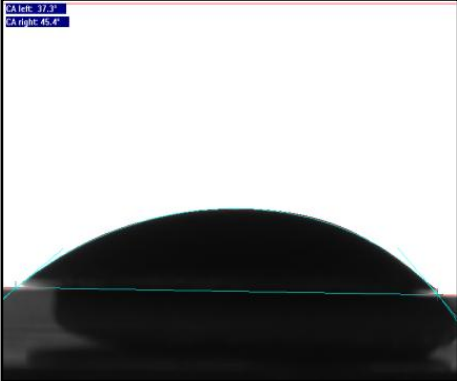
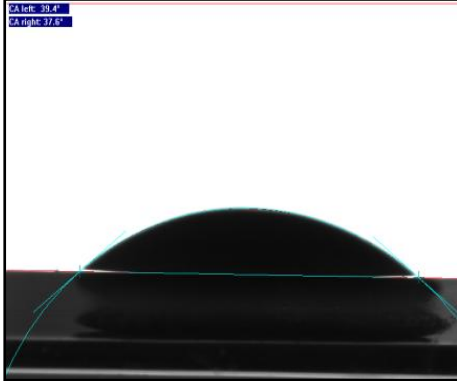
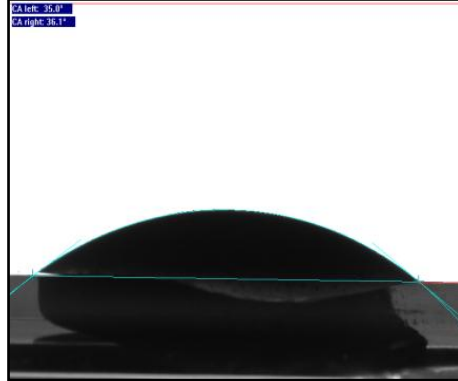
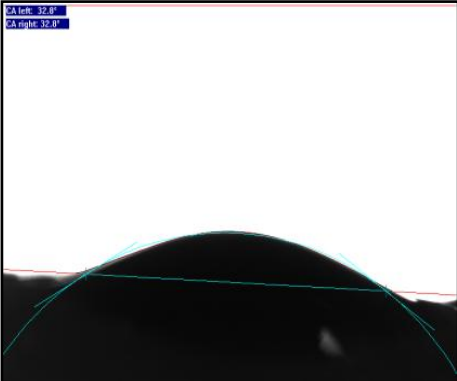
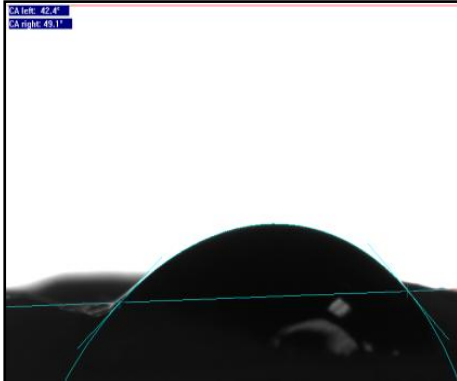
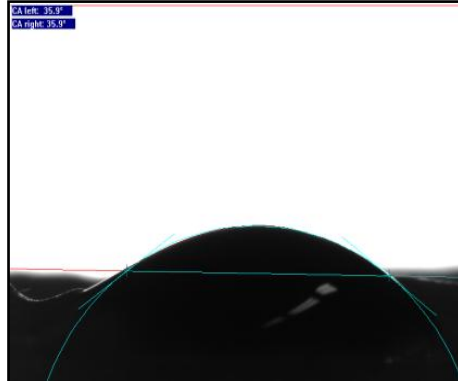
Types of surface	Run 1	Run 2	Run 3
On glass	 <p>CA = 37.3° – 45.4°</p>	 <p>CA = 39.4° – 37.6°</p>	 <p>CA = 35.0° – 36.1°</p>
On urea	 <p>CA = 32.8°</p>	 <p>CA = 42.4° – 49.1°</p>	 <p>CA = 35.9°</p>

Figure 5.16: Images from experiment for contact angle of mixture with 20% lignin on urea and glass surface

5.2.3 Impact Velocity on Droplet Spreading Behavior

For this work, the equilibrium contact angle that was used is 120° . From the result of simulation, it is observed that impact velocity affects the spreading behavior of the liquid-sulfur droplet. The specifications of the droplet maintains except for the velocity which has been increased to 1.5m/s and 3.0 m/s. Higher impact velocity induced the droplet to spread faster and has a bigger diameter. Before impact, the droplet has a spherical shape at velocity of 0.5m/s at $t = 0.5\text{ms}$. Droplet starts to spread upon impingement and a thin film forms on the surface, which develops and expands horizontally with a radial velocity higher than that before impact (Oukach et. al., 2010). As shown in Figure 5.21 and Figure 5.22, the diameter of the droplet increases rapidly as its thickness decreases.

When the droplet is run at a lower impact velocity i.e., 0.5m/s as shown in Figure 5.19, the droplet has the lowest spreading factor due to the effect of contact angle where it has higher surface energy. The time of spreading for the droplet is also very short. It can be observed that on a 'very rough' surface, the droplet does not spread further after $t = 2\text{ms}$ as can be seen in Figure 5.17. As can be seen in Figure 5.19(a) and Figure 5.19(b), the droplet starts to recoil at $t = 10\text{ms}$ as compared to the droplet with higher impact velocity where splashing of the droplet occurs. Oukach et. al. (2010) investigates the deformation behavior of a liquid droplet impacting a solid surface and in his report; a raised rim is formed on the droplet with lower velocity at the margin of the lamella. This is due to the surface tension forces causing the droplet to retract and recoils.

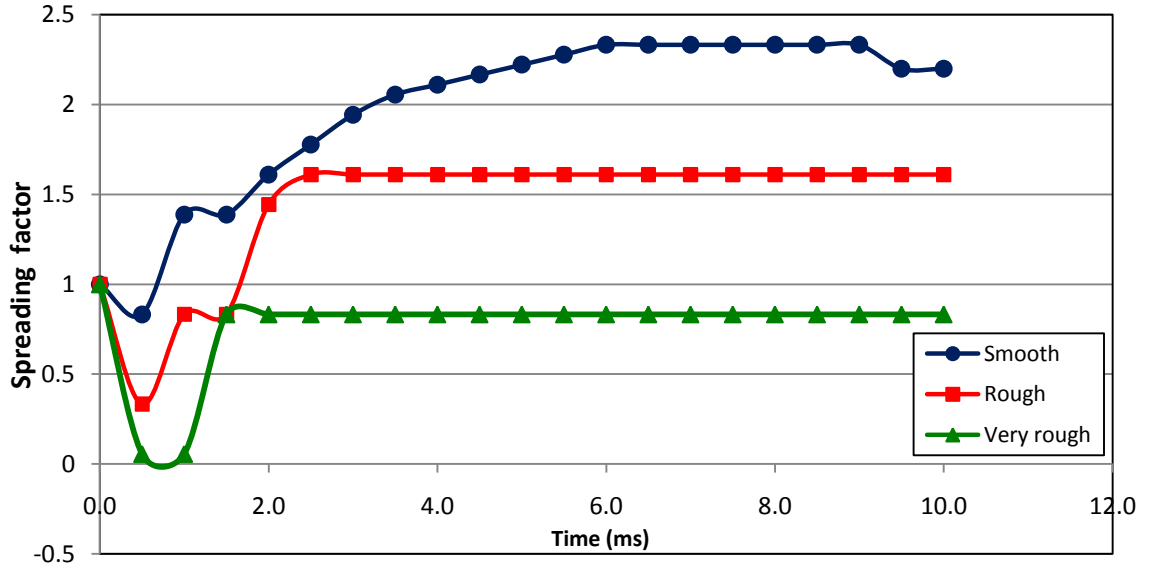


Figure 5.17: Spreading factor of droplet at velocity = 0.5m/s

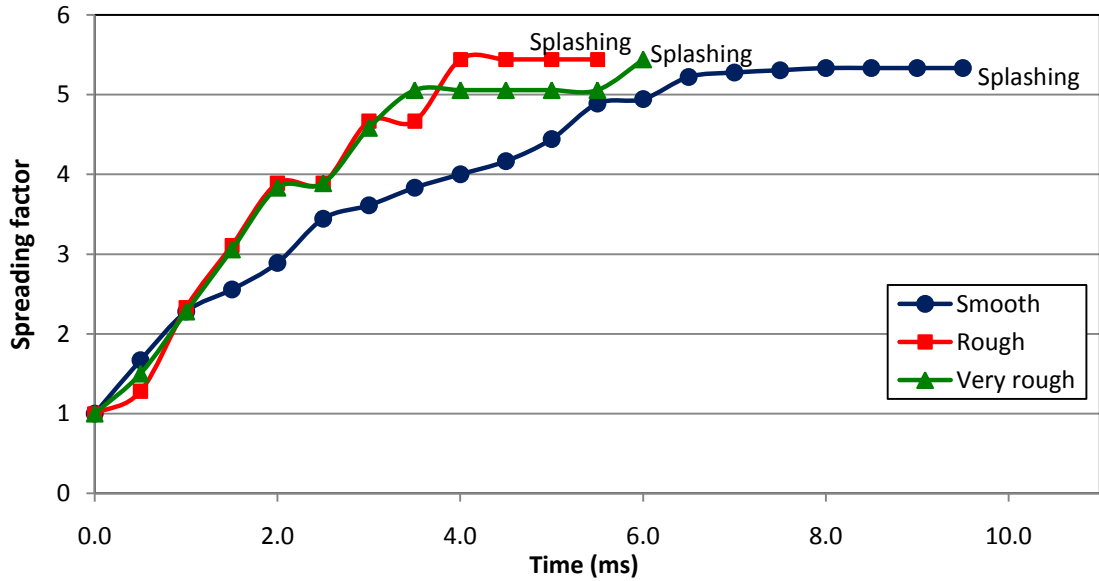


Figure 5.18: Spreading factor of droplet at velocity = 1.5m/s

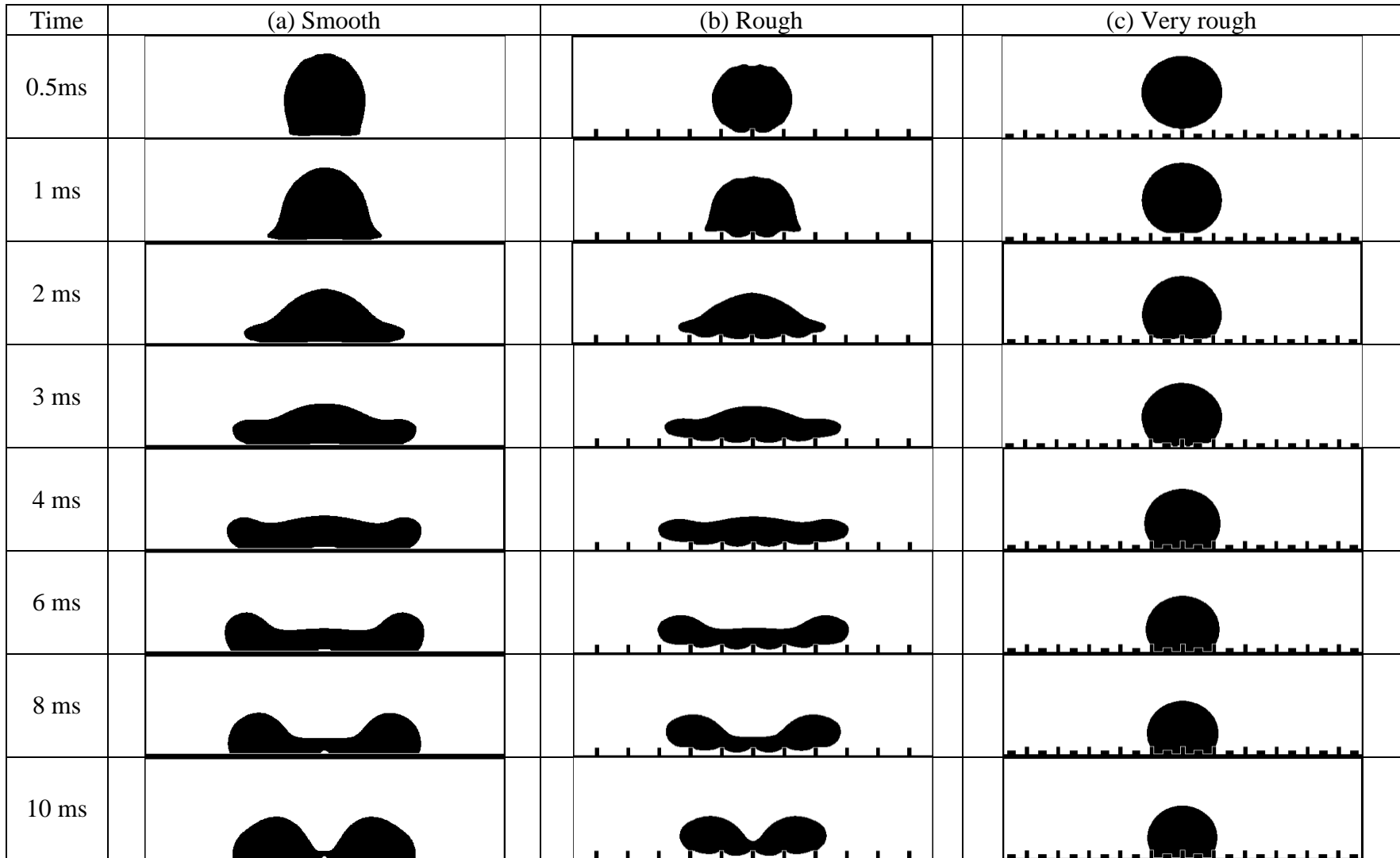


Figure 5.19: Droplet spreading behavior at velocity of 0.5m/s on different surface roughness

As can be seen from the graph in Figure 5.18, although the spreading factor has increased, the droplet starts to break up at 6 ms for rough surface, followed by very rough surface, and smooth surface but at a later time. In Figure 5.20, the droplet starts to breakup at $t = 3\text{ms}$ for rough surface; which is earlier by 50%. Splashing occurs in higher impact velocity as droplets are evicted from the rim of the lamella at the end of flattening. This is due to energy conservation where the kinetic energy exceeds the surface tension forces (Oukach et. al., 2010).

Generally, splashing would occur earlier in the droplet on ‘very rough’ surface, however, in this case, splashing occurs earliest on what was define as ‘rough’ surface. This is because the spaces between the textured surfaces of rough surface are bigger than that of the very rough surface. The spaces in between the textured surface on the very rough surface are smaller; therefore, the impact is cushioned by the surface and having lesser friction, leading to a delayed droplet splashing occurrence. The parameters of the textured surface were further discussed in Section 4.2 of Chapter 4.

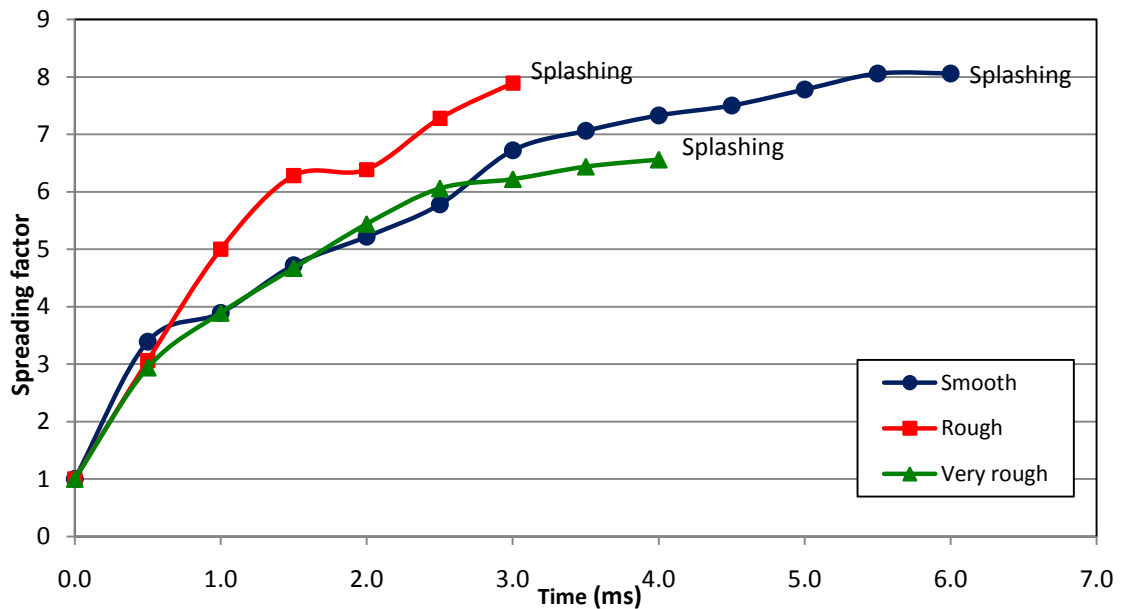


Figure 5.20: Spreading factor of droplet at velocity = 3m/s

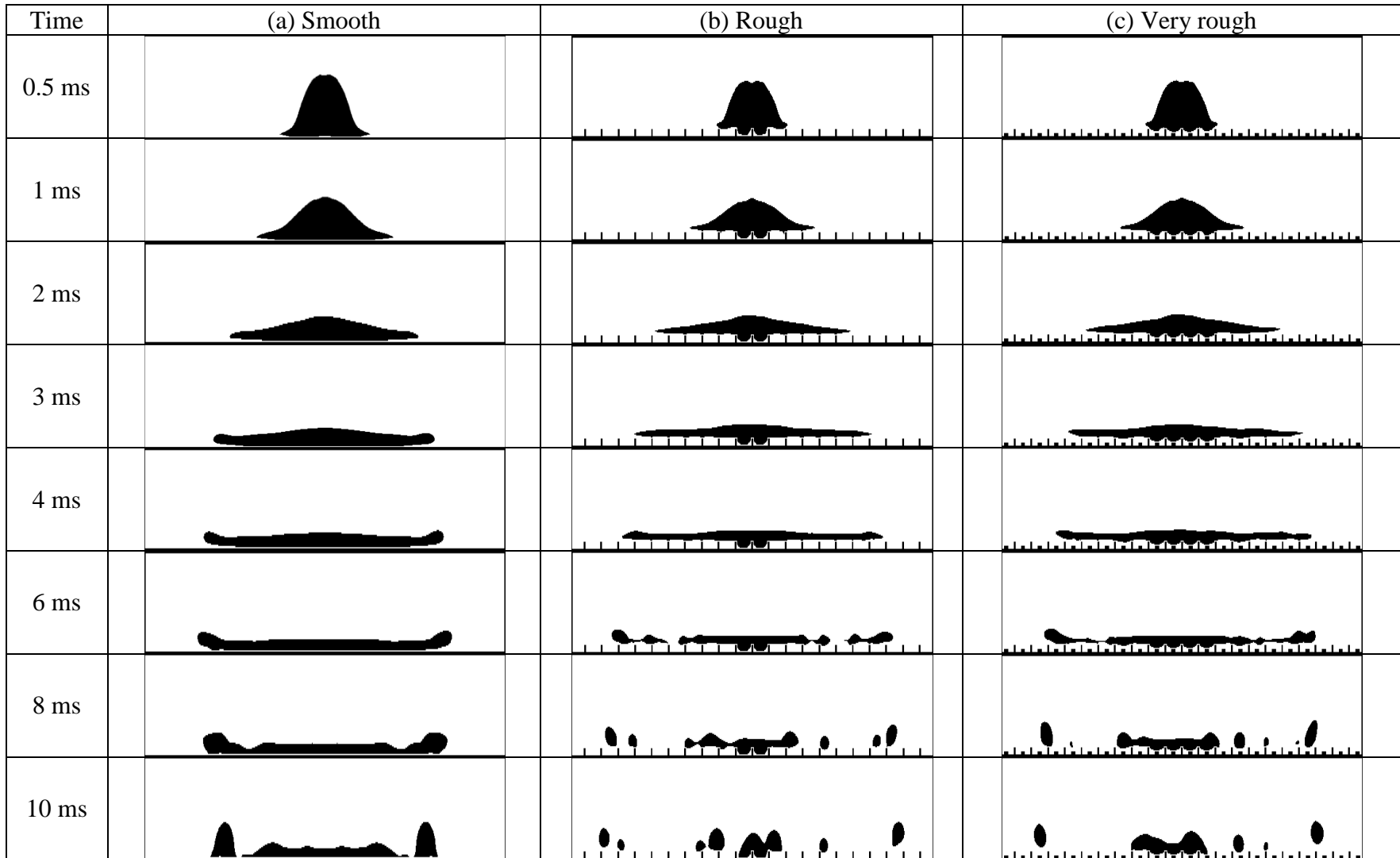


Figure 5.21: Droplet spreading behavior at velocity of 1.5m/s on different surface roughness

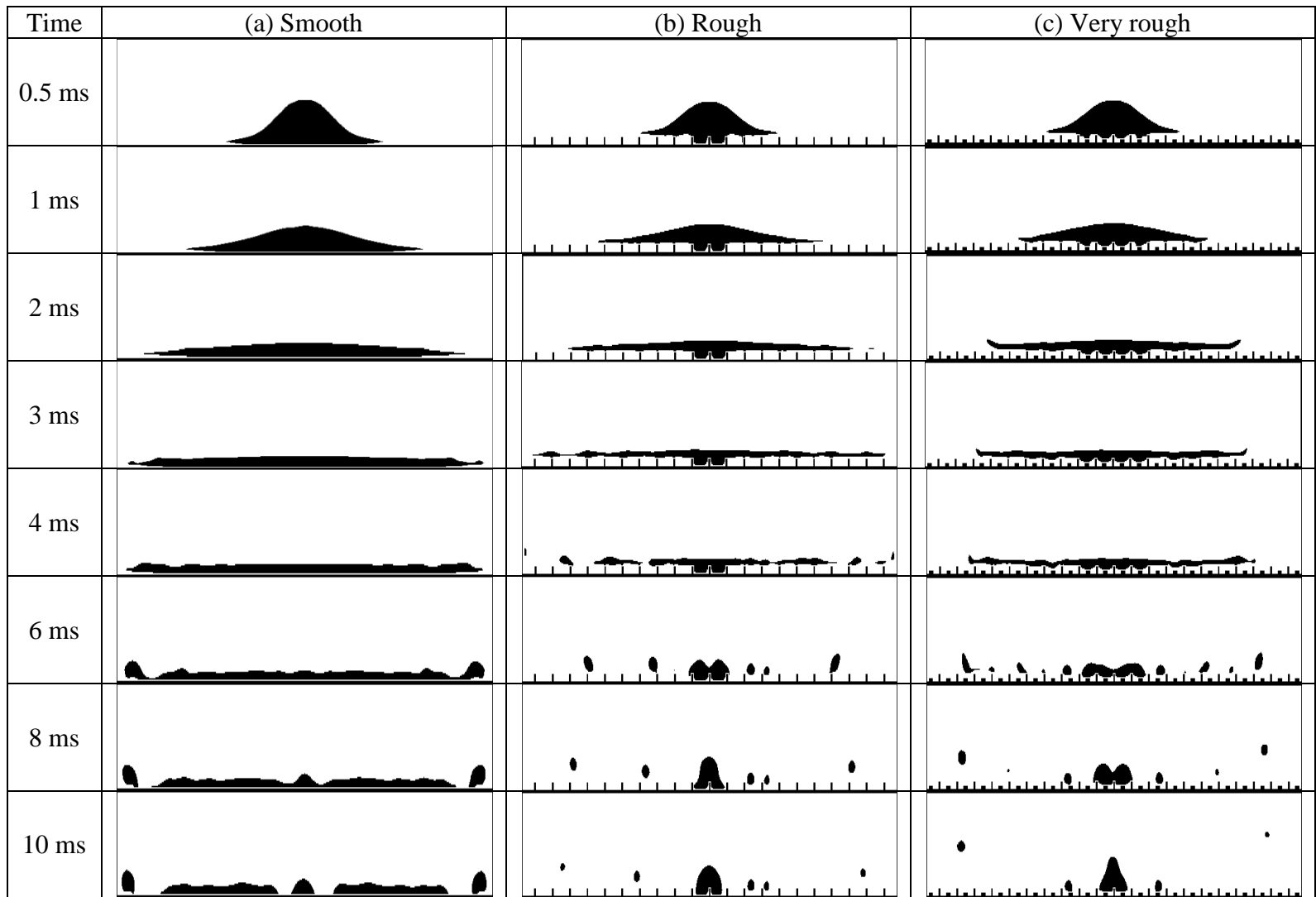


Figure 5.22: Droplet spreading behavior at velocity of 3.0m/s on different surface roughness

It should also be noted that wettability has an effect on the shape of the splat, particularly on the thickness and the maximum diameter and consequently on the spreading factor and spreading time. For a lower impact velocity i.e., 0.5m/s, the droplet recoils readily and rapidly, shortening the spreading time. As for high impact velocities the droplet spreads without recoil due to the kinetic energy exceeding the surface tension forces.

From this experiment, it can be deduce that increasing the velocity in urea coating process does not lead to desired urea coating as splashing may occur and a case of agglomeration will take place as reported by Link and Schlünder (1997) where destruction on wet surface leads to formation of new particle.

CHAPTER 6

CONCLUSION AND RECOMMENDATION

6.1 CONCLUSION

Prior to the simulation, grid size study was done to optimize running time for the simulation. From the results, it shows that time step of 1×10^{-07} is the best time step size and the grid size of 0.025mm x 0.025mm is the most favorable grid size to run the simulation.

As can be seen in the SEM images of urea, certain area of the urea appears to be smooth while certain area of the urea appears to be rough. A VOF multiphase model of 1.8mm droplet was developed to predict spreading behavior of a droplet on urea surface. Different surface roughnesses in the model were varied by creating different texture sizes in the domain. The simulation of the droplet spreading behavior on the different surface roughness was successfully simulated as it plays an important role because it cannot be determined in the fluidized bed where a droplet would be in contact with a urea, either on a smooth surface or on a rough surface since the approximate diameter of a urea is around 3.5 mm as shown in Figure 6.1, compared to the diameter of a droplet which is approximately 1.8 mm.

From the result in Section 5.2.1 in Chapter 5, very rough surface has higher surface area, followed by rough surface, and smooth surface. Mushroom state which is governed by the Wenzel model is also exhibited by the rough surface and very rough surface where droplet sits on small air pockets instead of penetrating entirely into the substrate. This is because the substrate is considered to be porous due to its surface roughness and also a heterogeneous surface, unlike the homogenous smooth surface.

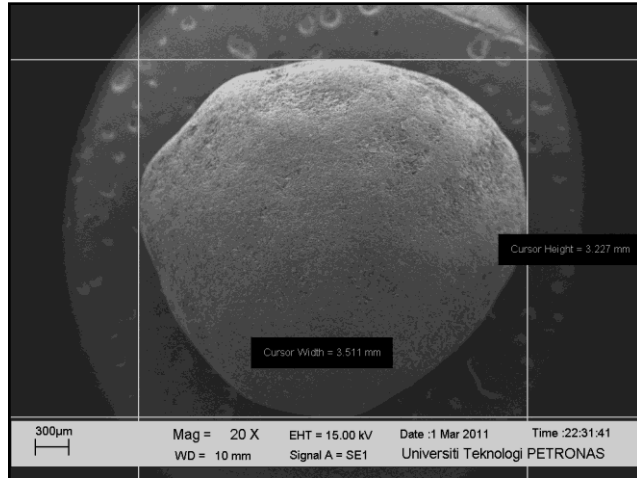


Figure 6.1: SEM image of urea with width and height of 3.511 mm and 3.227 mm; respectively

The effect of static contact angle was also investigated in this work. The contact angle of 30° gives the closest result to the experimental data provided by Zahirah (2011). Spreading factor is highest at a lower contact angle as it has lower surface energy while at a higher contact angle i.e., 120° droplet readily recoils and retracts which is in agreement with the findings of Oukach et. al. (2010). At $CA = 120^\circ$ and $CA = 60^\circ$, droplet on rough surface and very rough surface, respectively, exhibits the Cassie-Baxter model where air is trapped under the droplet. The high contact angle and the condition of the surface hinders the droplet from spreading further, creating a contact angle hysteresis where the contact angle advanced and then recede.

Another important point to be noted in this work is the velocity impact towards the droplet spreading behavior on the surface of urea. As mentioned by Link and Schlünder (1997), velocity plays a significant role to the extent of whether the urea would agglomerate or the droplet would spread on the urea. Splashing occurs earlier at the impact velocity of 3.0m/s, which is higher by 50% compared to the impact velocity of 1.5m/s. Kinetic energy exceeds the surface tension of the droplet, causing it to splash.

It should also be noted that splashing occurs earlier on a rough surface, compared to that of very rough surface. This is because the spaces between the textured surface of the very rough surface cushions the droplet from the high impact velocity, delaying the splashing of the droplet, whereas on the rough surface, the spaces of the textured surface is bigger. A velocity of 0.5 m/s proves to be sufficient to avoid any agglomeration or splashing of droplet as compared to the velocity of 1.5 m/s and 3.0 m/s which gives good agreement with the findings of Link and Schlünder (1997), where increasing the droplet velocity decreases the coating efficiency of particle.

In brief, time step size of 1×10^{-07} s and grid size of 0.025mm x 0.025mm is the optimal parameter to run the simulation. Droplet spreading behavior of sulfur droplet on surface of urea is successfully simulated using Fluent® where surface roughness has significant effect on droplet spreading, demonstrating a lower spreading factor. Lower contact angle increases droplet spreading diameter and high impact velocity leads to splashing as well as high spreading factor.

6.2 RECOMMENDATION & FUTURE WORK

The coating material that is used in the coating process can be improvised by using modified sulfur that utilizes a primary coating of sulfur and a secondary polymer coat, Sartain (2010). This type of coating provides a better uniformity in nutrient release compared to sulfur-coated urea as the rate of diffusion is controlled by the composition and thickness of polymeric film.

The extension of this work in the future could be developed to study the effect of sulfur droplet properties at different temperature i.e., 130°C as well as 140°C in the coating process of urea. Since urea is considered to be a porous and hydrophilic material, penetration of the droplet behavior and the evaporation of the droplet could be deliberated further in the future.

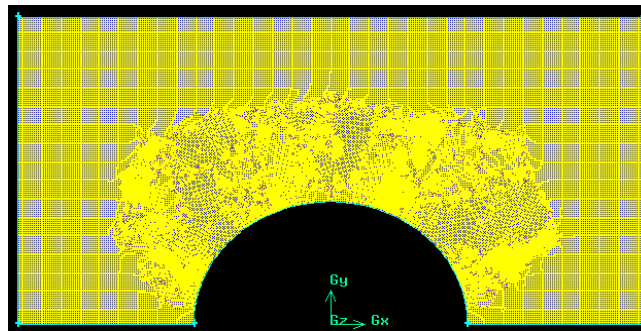


Figure 6.2: Meshed flow domain with a curvature on the horizontal axis

The surface of the flow domain is also of interest as it can be made into a semi-circle, impersonating the round shape of the urea as illustrated in Figure 6.2. Other than that, the space between the sulfur droplet and the horizontal wall (x-axis) can be specified at different coordinate to study the effect of different droplet height towards the spreading diameter. Alternatively, this can also be done by using a User Define Function (UDF) to input the velocity of the droplet to enable it to change with time.

REFERENCES

- Akelah, A., 1996, "Novel utilizations of conventional agrochemicals by controlled release formulations." *Mater. Sci. Eng.* **C4**, 83-98.
- Salman Omar, A. 1989, "Polyethylene-coated urea. 1. Improved storage and handling properties." *Ind. Eng. Chem. Res.* **28**, 630-632.
- S.S. Malhi, C.A. Grant, A.M. Johnston, K.S. Gill, 2001 "Nitrogen fertilization management for no-till cereal production in the Canadian Great Plains: a review" *Soil Tillage Res.* **60**, 101-112.
- Pipko, G., 1988 "Method for manufacture of slow-release fertilizers" EP 0276179
- Sartain, J. B., 2010, "Food for Turf: Slow Release Nitrogen" *University of Florida*
- Tomaszewska, M.; Jarosiewicz, A., 2002, "Use of Polysulfone in Controlled-Release NPK Fertilizer Formulations" *J. Agric. Food Chem.* **50**, 4634-4639
- Epstein, N. and Grace, J. R., 1984, "In *Handbook of Powder Science and Technology*", eds. L. Otten and M. E. Fayed, Chap. 11. Van Nostrand Reinhold, New York, U.S.A.
- Meisen, A. and Mathur, K. B., 1978, "Production of sulphur-coated urea by the spouted bed process." Paper presented at the 2nd International Conference on Fertilizers. *Proceedings of the British Sulfur Corporation -- Part I*, 3-6 December, pXIV, pp. 2-18.
- Link, C. and Schlünder, Ernst-Ulrich, 1997, "Fluidized bed spray granulation: Investigation of the coating process on a single sphere," *Chemical Engineering and Processing* **36**, 443-457
- Choi, M. S., and Meisen, A., 1996, "Sulfur coating of urea in shallow spouted beds" *Chemical Engineering Science*, Vol. 52 pp 1073-1086
- Turton, R., 2008, "Challenges in the modeling and prediction of coating of pharmaceutical dosage forms" *Powder Technology* **181**, 186-194

Rindt, D. W., Blouin, G. M. and Getsinger, J. G., 1968, "Sulfur Coating on Nitrogen Fertilizer to Reduce Dissolution Rate" *J. Agric. Food Chem.* **16**(5)

Weiss, P. J., 1981, "Spouted Bed Process for Sulfur Coating Fertilizers", *National University of Engineering*

Range, K., and Feuillebois, F., 1998, "Influence of Surface Roughness on Liquid Drop Impact," *Journal Of Colloid And Interface Science*, **203**, 16–30

Katagiri, K., Sato, T., and Nishiyama, H., 2005, "Spreading behavior of an impacting drop on a structured rough surface," *Physics Of Fluids*, **17**, 100608

Liu, Y. H., Wang, T. J., Qin, L., and Jin, Y., 2007, "Urea particle coating for controlled release by using DCPD modified sulfur," *Powder Technology*, **183**, 88-93

Ayub, G. S. E., Rocha, S. C. S., and Perucci, A. L. I., 2000, "Analysis of the Surface Quality of Sulfur-Coated Urea Particles in a Two-Dimensional Spouted Bed," *Brazilian Journal of Chemical Engineering*

FLUENT ©Inc. User's Guide, 2003, "Volume of Fluid (VOF) Model"

Doan, H. D., Trass, O., and Fayed, M. E., 1999, "Investigation of Urea Release from a Coated Sphere into a Quiescent Liquid," *Ind. Eng. Chem. Res.* **38**, 1125-1132

Weiss, P. J.; Meisen, 1983, "A. Laboratory Studies on Sulphur-Coating Urea by the Spouted Bed Process." *Can. J. Chem. Eng.* **61**, 440.

Ku-Shaari, K. Z., 2007, "Coating Uniformity in a pharmaceutical tablet: An experimental study and finite volume modeling of droplet impact behavior."

Timmons, R. J., 1987, "Sulfur Based Encapsulants for Fertilizers" *United States Patent*

Shirley, Jr., A. R., and Meline, R. S., 1975, "Sulfur-Coated Urea from a 1-Ton-Per-Hour Pilot Plant," *New Uses of Sulfur; West, J.; Advances in Chemistry*

Goertz et. al., 1993, "Sulfur Coated Fertilizers and Process For The Preparation Thereof," *U.S. Patent 5,219,645*

Gullett et. al., 1987, "Sulfur-Coated Urea," *U.S. Patent 4,676,821*

Lee, A. K. K., and Meisen, A., 1983, "Freeze-Coating Process for Producing Sulfur-Coated Urea," *Ind. Eng. Chem. Process Des. Dev.*, **22**, 503-509

Y. Ji et. al., 2011, "The diffusion coefficient of H₂S in Liquid Sulfur," *Fluid Phase Equilibria*

Di Lullo et. al., 2007, "Process For The Disposal Of Sulfur," *U.S. Patent 7,311,468 B2*

Ono, K., and Matsushima, T., 1957, "The Surface Tension of Liquid Sulfur," *The Research Institute of Mineral Dressing and Metallurgy*

Oukach et. al., 2010, "Deformation Behavior of a Liquid Droplet Impacting a Solid Surface," *COMSOL Conference 2010 Paris*

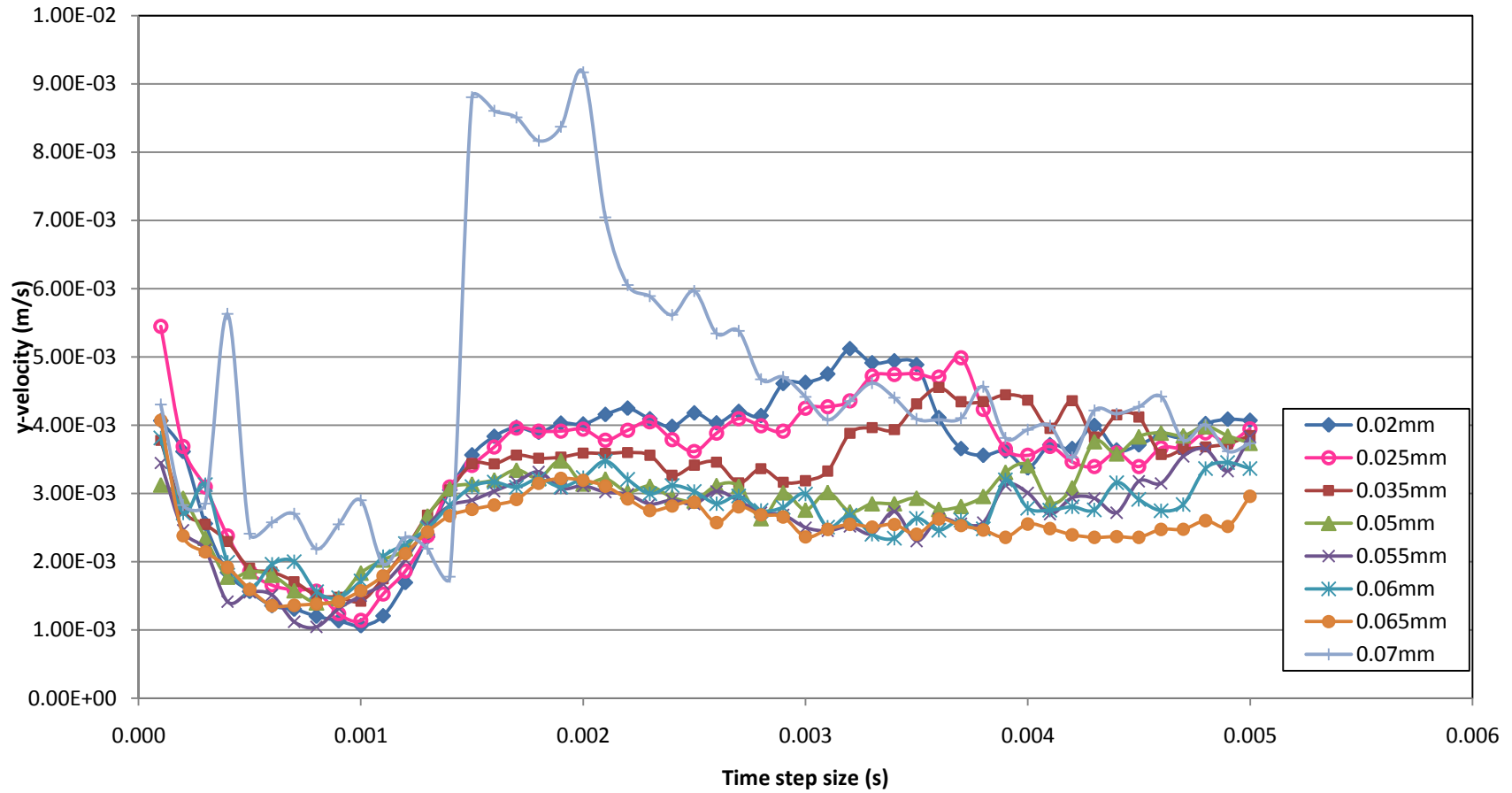
Bico, J., Thiele, U., and Que'r e', D., 2002, "Wetting of Textured Surfaces," *Colloids and Surfaces: Physicochemical and Engineering Aspects 206*, **41 – 46**

Whyman, G., Bormashenko, E., Stein, T., 2007, "The rigorous derivation of Young, Cassie–Baxter and Wenzel equations and the analysis of the contact angle hysteresis phenomenon," *Chemical Physics Letters 450* **355 – 359**

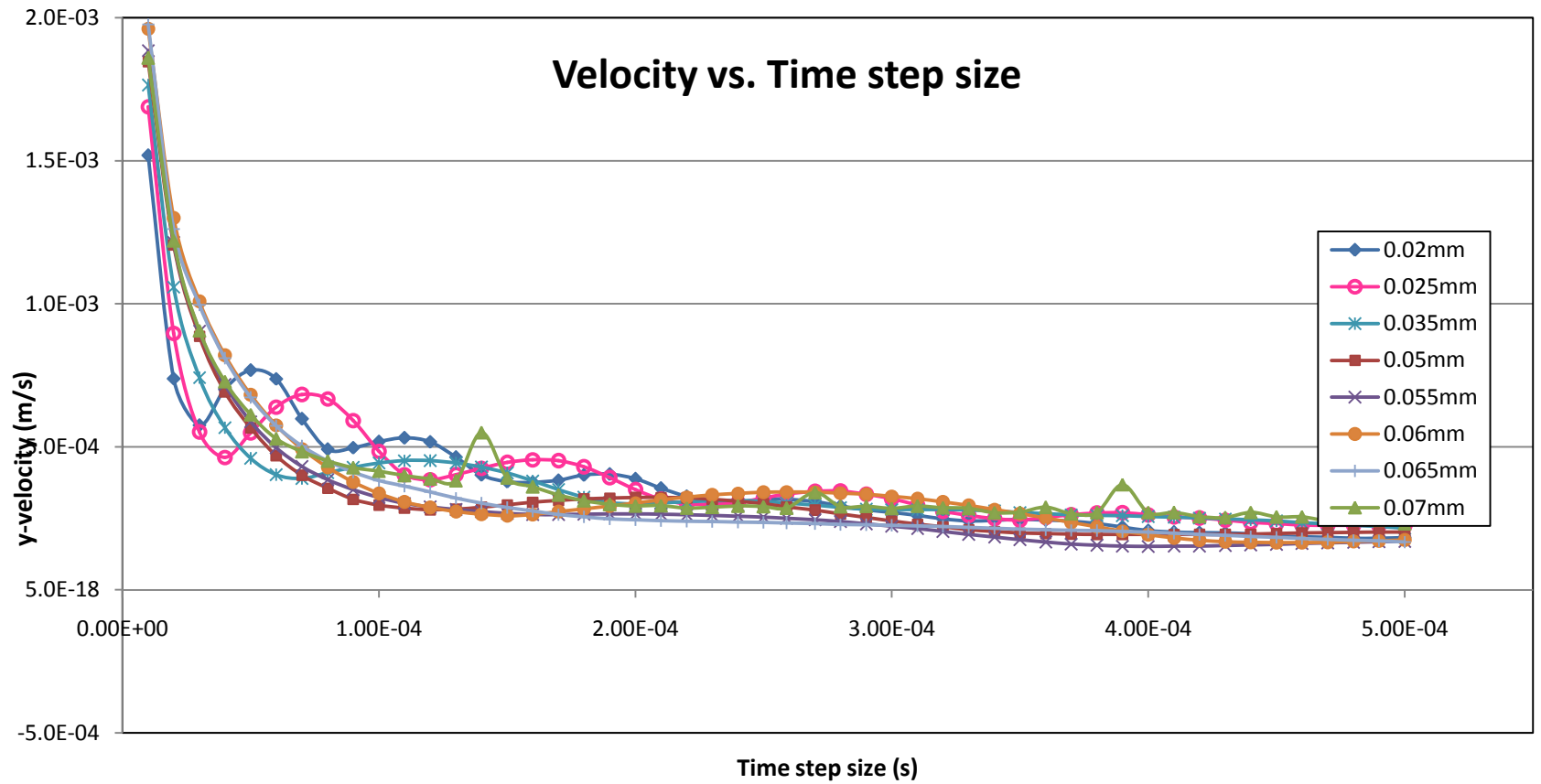
Zulhaimi, N. Z., 2011, "Study of Biomass Droplet Characteristics on Urea Surface"

APPENDICES

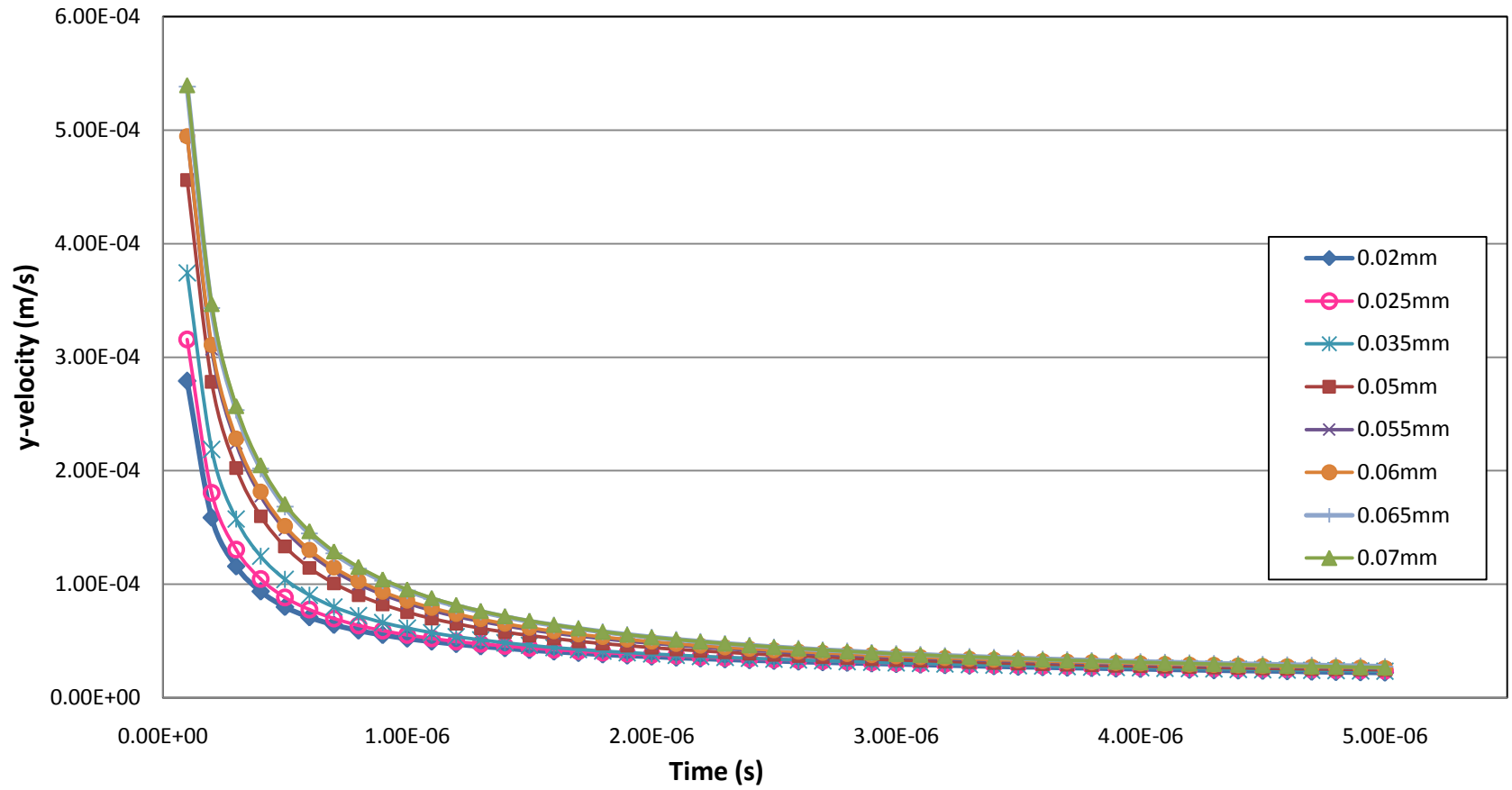
Velocity vs. Time step size



Appendix 1: Graph shows velocity against time for time step of 1×10^{-5} s



Appendix 2: Graph shows velocity against time for time step of 1×10^{-6} s



Appendix 3: Graph shows velocity against time for time step of 1×10^{-08} s